Amplification effects of news shocks through uncertainty

Danilo Cascaldi-Garcia*
Warwick Business School
University of Warwick
danilo.garcia.14@mail.wbs.ac.uk

November, 2017

JOB MARKET PAPER

Abstract

In this paper I investigate the empirical relationship between agents' responses to future technological improvements and the level of uncertainty in the economy. I show that the economic responses to news shocks change substantially over time, and that this dynamic couples with periods of high and low uncertainty. Periods of high uncertainty are characterized by higher positive economic effects of news shocks on output, consumption, investment and real personal income. These results indicate that the continuous updating of agents' expectations about the current and future economic situation operates as a transmission channel for news shocks, amplifying its positive outcomes.

Keywords: forecasting error variance, stochastic volatility, structural VAR, news shock, uncertainty shock.

JEL codes: E32, E44.

*Cascaldi-Garcia acknowledges financial support for this work from Capes-Brazil. I thank Ana Galvão, Lucio D'Aguanno, Roger Farmer, Anthony Garratt, Ingomar Krohn, James Mitchell, Roberto Pancrazi, Ivan Petrella, Thijs van Rens, Giovanni Ricco, Juan Gozzi Valdez and Marija Vukotić for their comments and suggestions.

1 Introduction

How do economic agents react to new information about future technological improvements? Although much has been done by the literature on business cycles driven by agents' beliefs to answer this question,[1] the results are not conclusive. Conventional wisdom is that the expectation of technological progress produces positive economic outcomes, but the empirical research still disagrees on the size and direction of this effect. In this paper, I show that a plausible reason for these differences is that agents react differently over time to news about technology. More importantly, these changes are intrinsically related to the degree of uncertainty about the economy.

The idea behind business cycles driven by 'news shocks' – changes in the future total factor productivity (TFP) that are foreseen by the economic agents (Beaudry and Portier, 2006) – is that technological innovations take time to have an impact in the economy. Part of this technological impact is foreseen by the economic agents, who react to it in the present. A new oil discovery is an example of a news shock.[2]

On an aggregate level, the literature on technological news shocks shows that positive news generates long-term co-movement among GDP, consumption and investment, and it is deflationary in the medium-term.[3] However, there is still an ongoing discussion, both theoretical and empirical, about (i) the extent to which this shock explains business cycles, (ii) how quickly one would observe an effect on productivity, and (iii) the effect on other important macroeconomic variables. For example, there is contradictory empirical evidence about the effect of a news shock on hours worked. While Beaudry and Portier (2006) show that a news shock generates a positive and significant effect on hours (consistent with the results from Christiano, Eichenbaum, and Vigfusson, 2003), Barsky and Sims (2011) present a negative effect of news on hours (in line with the technological

[1] See, for example, Beaudry and Portier (2006), Jaimovich and Rebelo (2009), Barsky and Sims (2011), Kurmann and Otrok (2013), Schmitt-Grohe and Uribe (2012), Blanchard, L'Huillier, and Lorenzoni (2013), Forni, Gambetti, and Sala (2014), Beaudry and Portier (2014), Levchenko and Pandalai-Nayar (2015), Vukotić (2017) and Cascaldi-Garcia and Galvao (2017).

[2] Although it will take years to be effectively explored, the expectation of future higher oil production induces the companies to invest now. Arezki, Ramey, and Sheng (2017) explore the news shock properties related to oil discoveries.

[3] As demonstrated by Beaudry and Portier (2006), Barsky and Sims (2011) and Beaudry and Portier (2014).

shock from Galí, 1999).

In fact, both results can be empirically observed just by changing the time-span of the estimation. Figure 1 presents the deciles of the impulse responses after a news shock identified over different periods in time, with a 20-year rolling window from 1975Q1 to 2012Q3. On average, the effect of a news shock on hours worked is positive in the medium-term, and negative in the long-term. However, depending on the identification period considered, the effect on hours can be positive in the medium-term and converging to zero, or zero in the medium-term and negative in the long-term.

Figure 1 Percentiles of responses to news shocks over different time periods

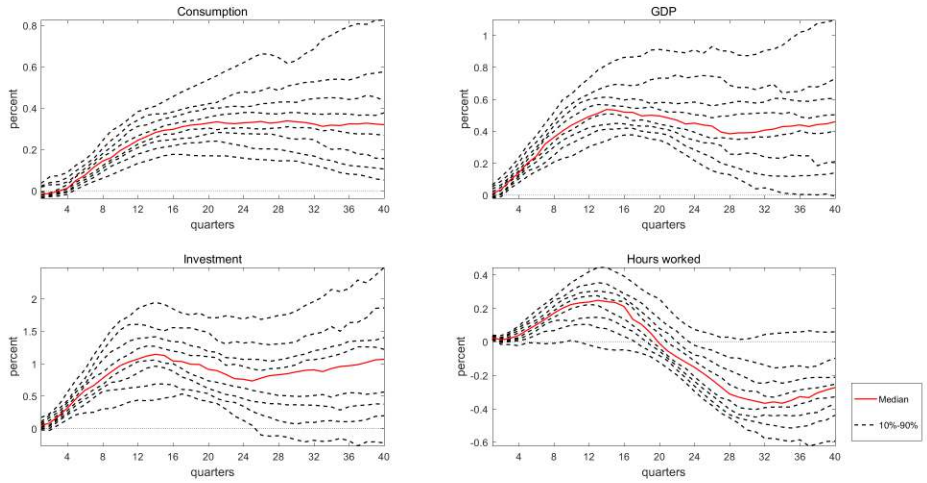

Note: Impulse responses of a news shock computed over a rolling window of 20 years, with quarterly data ranging from 1975Q1 to 2012Q3. The first window is from 1975Q1 to 1994Q4, while the last one is from 1992Q4 to 2012Q3. Each line corresponds to the deciles of the impulse responses calculated at the posterior mean from the 71 rolling window estimations, while the red line is the median. The identification follows the Barsky and Sims (2011) methodology, in a large Bayesian VAR consisting of the variables described in tables G.1 and G.2.

While the effect on hours worked changes both quantitatively and qualitatively, there are still differences in the size of the responses of real macroeconomic variables. Figure 1 shows that, on average, a news shock leads to a long-term positive effect on consumption, GDP and investment. However, depending on the time-span considered, this effect may be substantially stronger or converge to zero, with no long-term effects.

The economic effects of a news shock are far from robust to time changes. More broadly, these discrepancies show that the agents react to information about future tech-

nological improvements in different ways over time, and raises the question of whether such behavior is random or systemic. This question can be addressed by studying how the economic agents acquire information about future productivity, for example through the financial market.

Shen (2015) argues that agents are more responsive to information when signals are sufficiently precise. Uncertainty plays a role in how information is assimilated by the agents: information can be interpreted in different ways in periods of high or low uncertainty, indicating a potential amplifying effect of news shocks through an uncertainty transmission channel.

The rolling window identification exercise supports this relationship between news about future productivity and uncertainty. Figure 2 presents the long-term effects of a news shock on consumption identified in a 20-year rolling window, and compares it with a measure of macroeconomic uncertainty.[4] There is a clear period of high long-term effects until 2001, followed by a period of low long-term effects, increasing again after 2007. This behavior is systematic, and matches with periods of high and low macroeconomic uncertainty.

In this paper, I propose a model and identification procedure to investigate whether agents change the way they respond to news about future productivity over time, and if this behavior depends on economic uncertainty. Investigating for heterogeneous responses over time means that the news shock identification should allow for nonlinear and time-varying models. Investigating for the interaction between uncertainty and news shocks means that such a model should be flexible enough to capture systemic changes in the economic responses to a news shock based on the level of uncertainty.

The premise of the model is that uncertainty measures the agents' expectations about current and future economic conditions. It is reasonable to think that these expectations should also be updated when the agents receive news about future higher productivity. In other words, the level of uncertainty *endogenously* responds to exogenous news shocks. To meet these requirements, I employ a stochastic volatility model that treats macroeconomic

[4]Macroeconomic uncertainty measure calculated by Ludvigson, Ma, and Ng (2016).

Figure 2 Long-term effects of a news shock on consumption and macroeconomic uncertainty

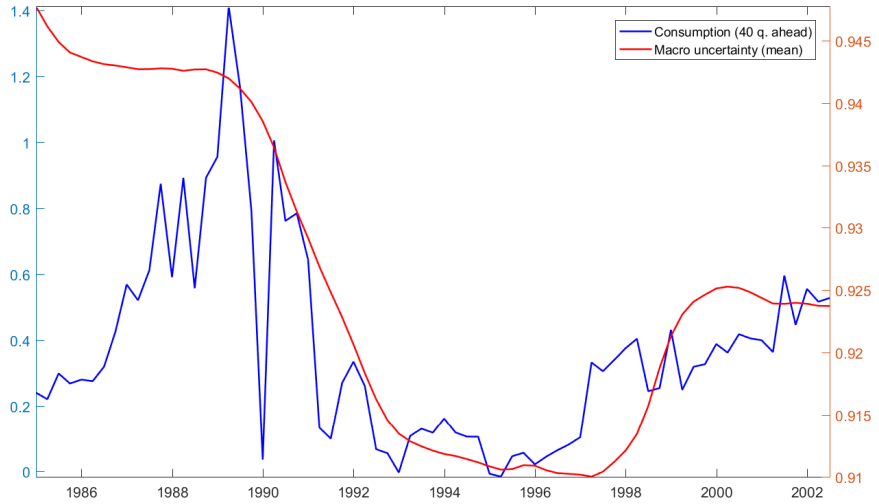

Note: In red: Mean of a macroeconomic uncertainty measure calculated by Ludvigson et al. (2016). In blue: Long-term effects of a news shock on consumption. Long-term defined as 40 quarters ahead of the news shock. The news shock is computed over a rolling window of 20 years, with quarterly data ranging from 1975Q1 to 2012Q3. The first window is from 1975Q1 to 1994Q4, while the last one is from 1992Q4 to 2012Q3. The x-axis shows the mid-point of the window. The identification follows the Barsky and Sims (2011) methodology, in a large Bayesian VAR consisting of the variables described in tables G.1 and G.2.

and financial uncertainties as latent variables.

The baseline model builds upon Carriero, Clark, and Marcellino (2016a), as a nonlinear stochastic volatility Bayesian vector autoregressive (VAR) model for large datasets. With this structure, it is possible to identify first moment shocks, as news shocks, allowing for unrestricted interrelationship between the first and second moments of the data. The estimated volatilities are divided into two components: an idiosyncratic and a common component. The common component is either a latent factor across all macroeconomic variables included in the VAR, or across all financial variables. These common factors are the *proxies* for macroeconomic and financial uncertainties. The common volatility factors are included in the VAR, contemporaneously affecting the conditional mean of the variables. Finally, the common volatility factors also depend on the lagged variables, creating a complete nonlinear feedback effect between first and second moments of the variables.

I also propose an identification method for news shocks that extends the current standard procedure for nonlinear and time-varying cases. The identification method is a generalization of the Barsky and Sims (2011) procedure of maximizing the variance decomposition of utilization-adjusted TFP over a predefined forecast period. Instead of assuming a constant variance, the identification procedure proposed here explicitly accounts for potential changes of the total forecast error variance at each point in time. Moreover, I modify the identification strategy such that it takes into account the nonlinear relationship between variables and their volatilities (volatility in mean) through the construction of generalized impulse response functions.

I bring two contributions to the empirical literature on measuring the economic effects of news shocks. First, I evaluate whether the impact of a news shock changes over time and whether the theoretical assumption of positive co-movement[5] holds in different periods. The evidence provided here of heterogeneous responses over time indicates that news shock identifications based on processes with time invariant covariances may not be appropriate.

Second, I show that news shocks interact with uncertainty. The results indicate that there is a close link between the arrival of information about future productivity and how this information is absorbed by the agents. This information is interpreted in different ways in periods of high or low uncertainty, influencing the impact of the news. The positive economic effects led by technology news are systematically higher in periods of high uncertainty, depending on the initial degree of uncertainty (level effect) and on how agents update their expectations about macroeconomic and financial conditions (transmission effect).

These results are consistent with Bloom (2009)'s interpretation of an overshooting of productivity in the medium-term after a period of high uncertainty. Productivity grows as firms address their pent-up demand for investments, and substitute less flexible for more flexible capital (Comin, 2000). Cascaldi-Garcia and Galvao (2017) show that high uncertainty increases the likelihood of news shocks, creating a 'good uncertainty' effect.

[5]Beaudry and Portier (2006).

This paper is aligned with literature about the relationship between news shocks and financial markets. Beaudry and Portier (2006) and Barsky and Sims (2011), for example, show how the stock market reacts to news shocks. Kurmann and Otrok (2013), Cascaldi-Garcia (2017) and Kurmann and Sims (2017) debate the effect of a news shock on short and long-term interest rates. Görtz, Tsoukalas, and Zanetti (2016) present the role of news shocks in light of propagation through frictions in financial intermediation. This paper also relates to an extensive literature on stochastic volatility VAR models. Mumtaz and Zanetti (2013), for example, allow for a lagged feedback of the volatilities to the mean. Alessandri and Mumtaz (2014), Shin and Zhong (2016) and Carriero, Clark, and Marcellino (2016b) propose models with a contemporaneous feedback of a common volatility factor to the mean.

The outline of the paper is as follows. I present the underlying model that allows for stochastic volatility in mean and the estimation procedure in Section 2. Section 3 introduces an identification procedure for the news shock that takes into account nonlinear and time-varying models, and a procedure for identifying uncertainty shocks. Section 4 presents the estimated latent macro and financial uncertainty measures. Section 5 summarizes the results for a news shock and its relations with uncertainty measures, while Section 6 describes the results of macroeconomic and uncertainty shocks. Section 7 concludes this paper.

2 A stochastic volatility in mean model

The empirical model aims at allowing a full interaction between uncertainty and macroeconomic variables so that orthogonal shifters of first and second moments can be identified. The proposed model setup is a large heteroskedastic VAR built upon Carriero et al. (2016a), in which the individual volatilities are a combination of a common uncertainty factor and an idiosyncratic volatility component. I modify its baseline framework to handle variables in levels. The choice of two common factors follows the recent literature on unobserved uncertainty components as a way of separating macroeconomic and financial

sources of uncertainty (Jurado, Ludvigson, and Ng, 2015 and Carriero et al., 2016a).

The non-observed macroeconomic and financial factors (*proxies* for macro and financial uncertainties) are included in the conditional mean of the VAR, which allows for a contemporaneous effect on the variables. In addition, the factors are dependent on the lagged variables, permitting a nonlinear feedback of the variables on their volatilities.

2.1 Model description

The model is estimated as a structural nonlinear VAR, with y_t representing a $(n \times 1)$ vector that stacks the n_m macroeconomic endogenous variables $y_{m,t}$ and the $n_f = n - n_m$ financial endogenous variables $y_{f,t}$, in levels, as in $y_t = (y_{m,t}; y_{f,t})$. g_t is a (2×1) vector that stacks the non-observed macroeconomic and financial uncertainty factors, denoted as $g_t = (\ln m_t; \ln f_t)$. Here renamed as 'Main VAR' for notation purposes, the model is represented under the reduced form

$$y_t = \mathbf{A}_1 y_{t-1} + ... + \mathbf{A}_p y_{t-p} + \mathbf{B}_0 g_t + ... + \mathbf{B}_l g_{t-l} + v_t, \tag{1}$$

where $\mathbf{A}_i$ are $(n \times n)$ matrices that collect the coefficients of the lags of y_t from 1 to p, $\mathbf{B}_i$ are $(n \times 2)$ matrices that collect the coefficients of the lags of g_t from 0 to l. This setup is similar to a VAR-X configuration, where g_t is modeled as an exogenous component.

The reduced form shocks v_t are modeled as

$$v_t = \mathbf{A}_0^{-1} \mathbf{\Lambda}_t^{1/2} \epsilon_t, \quad \epsilon_t \sim iid\ N(0, I), \tag{2}$$

where $\mathbf{A}_0$ is a lower $(n \times n)$ triangular matrix with ones in the main diagonal, and $\mathbf{\Lambda}_t$ is the time-varying $(n \times n)$ diagonal matrix that collects the variance of each variable. Each element of $\mathbf{\Lambda}_t$ is composed of an idiosyncratic component and a common uncertainty factor, which may be macroeconomic or financial depending on the chosen variable. The first n_m variables form the macroeconomic factor measure, while the $n_f = n - n_m$ variables

form the financial factor measure. The elements of $\mathbf{\Lambda}_t$ (in logs) are defined as

$$\ln \lambda_{j,t} = \begin{cases} \beta_{m,j} \ln m_t + \ln h_{j,t} & \text{if } j = 1, ..., n_m \\ \beta_{f,j} \ln f_t + \ln h_{j,t} & \text{if } j = n_m + 1, ..., n \end{cases}, \tag{3}$$

where $\beta_{m,j}$ and $\beta_{f,j}$ are the individual loadings to the common macroeconomic and financial factors, respectively. For identification purposes, I set $\beta_{m,1} = 1$ and $\beta_{f,n_m+1} = 1$.

The common macroeconomic factor is part of the volatility of all macroeconomic variables, and the financial factor is part of the volatility of the financial variables. The idiosyncratic component $\ln h_{j,t}$ follows an $AR(1)$ process of the form

$$\ln h_{j,t} = \gamma_{j,0} + \gamma_{j,1} \ln h_{j,t-1} + e_{j,t}, \quad j = 1, ..., n, \tag{4}$$

where $e_t = (e_{1,t}, ..., e_{n,t})'$ is jointly and independently distributed as $iid\ N(0, \mathbf{\Phi_e})$, and $\Phi_e = diag(\phi_1, ..., \phi_n)$.

I define the common macroeconomic and financial volatility factors as *proxies* for macroeconomic and financial uncertainty measures, respectively. These uncertainty measures $g_t = (\ln m_t; \ln f_t)$ also follow a VAR structure, and is referred to as 'Uncertainty VAR' for notation purposes. The Uncertainty VAR is modeled as

$$g_t = \mathbf{D}_1 g_{t-1} + ... + \mathbf{D}_k g_{t-k} + \delta \Delta y_{t-1} + u_t, \tag{5}$$

where $\mathbf{D}_i$ are (2×2) matrices that collect the coefficients of the lags of the uncertainty factors g_t from 1 to k. δ is a $(2 \times n)$ matrix that collects the coefficients of the lagged variables y_t (in differences). The shocks to the uncertainty factors $u_t = (u_{m,t}; u_{f,t})$ are independent from e_t and ϵ_t, with mean 0 and full covariance matrix defined as

$$\Phi_u = \begin{bmatrix} \phi_{n+1} & \phi_{n+3} \\ \phi_{n+3} & \phi_{n+2} \end{bmatrix}. \tag{6}$$

The covariance matrix of the uncertainty measures is purposely constructed as full,

to allow for co-movement between macroeconomic and financial uncertainty measures. I adapt the model structure by using lagged y_t variables in differences and not in levels. Carriero et al. (2016a) present a rich discussion on the suitability of this structure for identifying macroeconomic and financial uncertainties, and how this setup relates to the stochastic volatility literature.

The model embeds the assumption that uncertainty measures are affected by feedback from the lagged variables, and that uncertainty measures have a contemporaneous effect on the mean of the variables. It is not possible to have contemporaneous feedback to and from uncertainty simultaneously, for identification reasons. The choice of contemporaneous (and not lagged) feedback from uncertainty to the mean follows the assumption that the economic variables rapidly react to uncertainty shocks, and uncertainty causes short-term economic fluctuations (Bloom, 2009).

This setup imposes the limitation that shocks to the mean of the variables can only influence the level of uncertainty with, at least, one lag. One obvious alternative would be to assume that uncertainty measures are affected contemporaneously by the variables, and that uncertainty measures have a lagged effect on the mean of the variables. However, under such an assumption, economic variables would only react to uncertainty shocks after one lag. This seems implausible in a quarterly data information set, especially with respect to financial variables such as stock prices.

The non-observed idiosyncratic volatilities $h_{j,t}$ are estimated by the standard algorithm proposed by Kim, Shephard, and Chib (1998), using a 10-state mixture of normals approximation from Omori, Chib, Shephard, and Nakajima (2007). The estimation of the non-observed macroeconomic and financial uncertainties is substantially more complex, presenting a multi-variate nonlinear state-space representation. I follow Mumtaz and Theodoridis (2015) and employ a particle Gibbs step to estimate $\ln m_t$ and $\ln f_t$. The particle Gibbs construction is based on Andrieu, Doucet, and Holenstein (2010) and the ancestor sampling improvements proposed by Lindsten, Jordan, and Schön (2014), with 100 particles.

I estimate the full model with $p = 4$ lags, $l = 1$ lag of the macro and financial factors

in the Main VAR (equation 1), and $k = 1$ lag of the macro and financial factors in the Uncertainty VAR (equation 5). The full estimation procedure is described in detail in the Appendices.[6]

2.2 Data

The dataset comprises both macroeconomic and financial variables in levels. The variables are measured quarterly, which allows the use of macroeconomic variables such as utilization-adjusted TFP (necessary for the news shock identification) and gross domestic product (GDP). For variables which are available at a higher frequency, I construct the time-series by taking the quarterly average. The period is from 1975Q1 to 2012Q3.

The dataset contains 14 macroeconomic variables, namely utilization-adjusted TFP, personal consumption per capita, GDP per capita, private investment per capita, hours worked, GDP deflator, Federal funds rate, total nonfarm payroll, industrial production index, help wanted to unemployment ratio, real personal income, real manufacturing and trade sales, average of hourly earnings (goods producing) and producer price index (finished goods). These are the macroeconomic variables that are usually considered in the news shock literature.

The 14 financial variables are the spread between the 10-year yield and the Federal funds rate, S&P500 stock prices index, S&P dividend yields, excess bond premium, CRSP excess returns, small-minus-big risk factor, high-minus-low risk factor, momentum, small stock value spread (R15-R11), and five industry sector-level returns (consumer, manufacturing, high technology, health and other). The financial variables mostly matches those used by Jurado et al. (2015) and Carriero et al. (2016a) to construct their measures of financial uncertainty.

A full description of the sources and construction of the 28 variables can be found in Appendix G.

[6]Appendix A describes the triangularization procedure for drawing the coefficients in large VARs proposed by Carriero, Clark, and Marcellino (2016c). This procedure is statistically equivalent to a conventional Bayesian stochastic volatility Monte Carlo Markov Chain (MCMC) estimation, but has the advantage of being less computationally intensive. Appendix B presents the steps of the MCMC algorithm. Appendix C describes the particle Gibbs with ancestor sampling.

3 Identification procedure for news and uncertainty shocks

In this Section I present the strategy for identifying news and uncertainty shocks. These procedures can be considered as two separate computation methods, one time-varying and the other is time-invariant. The first is an innovative identification procedure for news shocks that takes into account nonlinear and time-varying models, in which the news shock presents different economic responses in each point in time. The second is a standard generalized impulse response procedure for macroeconomic and financial uncertainty shocks. Since the latent macro and financial factors have time invariant covariances, the identification procedure is also invariant over time.

3.1 News shocks identification for nonlinear and time-varying models

The identification for the news shock is constructed upon the procedure proposed by Barsky and Sims (2011). This approach is based on the assumption that a technology news shock is the structural shock that best explains the unpredictable movements of utilization-adjusted TFP over a fixed long-term horizon,[7] with the imposition of no effect on impact ($t = 0$). It is constructed following the maximum forecast error variance approach presented in Uhlig (2005) and Francis, Owyang, Roush, and DiCecio (2014).

The identification procedure presented by Barsky and Sims (2011) is broadly adopted in the news shock literature.[8] However, this identification method is only applicable to time invariant covariance cases. A more flexible identification method is needed to investigate the idea of an underlying transmission mechanism relating the technology news (a shock to the mean of the variables) and the variables' volatilities.

I start from the model presented in equation 1. Considering a model with a fully

[7] I follow Barsky and Sims (2011) by fixing the horizon at 40 quarters ahead.

[8] For example, Coibion and Gorodnichenko (2012), Kurmann and Otrok (2013), Forni et al. (2014), Ben Zeev and Khan (2015), Görtz et al. (2016) and Cascaldi-Garcia and Galvao (2017). See Beaudry and Portier (2014) for an extensive discussion about identification methods for news shocks.

exogenous uncertainty measure g_t, I rewrite equation 1 as a function of the lag operator L, leading to a VAR-X representation of the form

$$y_t = \mathbf{A}(L)y_t + \mathbf{B}(L)g_t + \mathbf{A}_0^{-1}\mathbf{\Lambda}_t^{1/2}\epsilon_t, \tag{7}$$

where $\mathbf{A}(L) = \mathbf{A}_1 L + \mathbf{A}_2 L^2 + ... + \mathbf{A}_p L^p$ and $\mathbf{B}(L) = \mathbf{B}_0 + \mathbf{B}_1 L + ... + \mathbf{B}_l L^l$. A moving average representation of this model[9] is defined as the infinite polynomial of the lag operator L as $\mathbf{C}(L) = \mathbf{C}_0 + \mathbf{C}_1 L + ... = [\mathbf{I}_n - \mathbf{A}(L)]^{-1}$, where $\mathbf{C}_0 = \mathbf{I}_n$, as

$$y_t = \mathbf{C}(L)\mathbf{B}(L)g_t + \mathbf{C}(L)\mathbf{A}_0^{-1}\mathbf{\Lambda}_t^{1/2}\epsilon_t. \tag{8}$$

Suppose that there is a linear mapping of the innovations (ϵ_t) and the structural shocks (s_t) as in

$$\epsilon_t = \mathbf{P}s_t, \tag{9}$$

which implies

$$\mathbf{A}_0^{-1}\mathbf{\Lambda}_t^{1/2}\epsilon_t = \mathbf{A}_0^{-1}\mathbf{\Lambda}_t^{1/2}\mathbf{P}s_t. \tag{10}$$

The innovations ϵ_t and the structural shocks s_t are i.i.d. $N(0, \mathbf{I}_n)$. To ensure that $\mathbb{E}[\mathbf{A}_0^{-1}\mathbf{\Lambda}_t^{1/2}\epsilon_t\epsilon_t^{'}\mathbf{\Lambda}_t^{1/2'}\mathbf{A}_0^{-1'}] = \mathbb{E}[\mathbf{A}_0^{-1}\mathbf{\Lambda}_t^{1/2}\mathbf{P}s_t s_t^{'}\mathbf{P}'\mathbf{\Lambda}_t^{1/2'}\mathbf{A}_0^{-1'}] = \mathbf{\Sigma}_t$, it suffices that $\mathbf{P}\mathbf{P}' = \mathbf{I}_n$. $\mathbf{P}$ can take the form of any of the infinite alternatives that satisfy this condition. Under this structure, the moving average representation can be rewritten as

$$y_t = \mathbf{C}(L)\mathbf{B}(L)g_t + \mathbf{C}(L)\mathbf{A}_0^{-1}\mathbf{\Lambda}_t^{1/2}\mathbf{P}s_t, \tag{11}$$

where $s_t = \mathbf{P}^{-1}\epsilon_t$.

Now, the Barsky and Sims (2011) identification procedure for the news shock relies on finding one of the infinite alternatives of $\mathbf{P}$ that maximizes the variance decomposition of the utilization-adjusted TFP over a predefined forecast horizon, and has no effect on impact ($t = 0$). It is derived from the assumption that technology is a stochastic

[9]See Ocampo and Rodríguez (2012) for a comprehensive description of the moving average representation of VAR-X models.

process driven by two shocks: a surprise (or unanticipated) technological shock, and an anticipated news shock. The total unexplained variance of utilization-adjusted TFP can be decomposed as

$$\Gamma_{1,1}(k)_{surprise} + \Gamma_{1,2}(k)_{news} = 1 \forall h, \tag{12}$$

where $\Gamma_{i,j}(h)$ is the share of the forecast error variance of variable i of the structural shock j at horizon k, $i = 1$ refers to utilization-adjusted TFP (where this variable is ordered first in the VAR), $j = 1$ is the unexpected TFP shock, and $j = 2$ is the news shock.

While the K-step ahead forecast error in this model is given by

$$y_{t+K} - \mathbb{E}[y_{t+K}] = \sum_{k=0}^{K} (\mathbf{C}_k \mathbf{B}_k g_{t+k} + \mathbf{C}_k \mathbf{A}_0^{-1} \mathbf{\Lambda}_{t+k}^{1/2} \mathbf{P} s_{t+K-k}), \tag{13}$$

the share of the forecast error variance of the news shock is

$$\begin{aligned} \Gamma_{1,2}(K)_{t,news} =& \frac{q_1' \left(\sum_{k=0}^{K} (\mathbf{C}_k \mathbf{B}_k g_{t+k} + \mathbf{C}_k \mathbf{A}_0^{-1} \mathbf{\Lambda}_{t+k}^{1/2} \mathbf{P} q_2)(\mathbf{C}_k \mathbf{B}_k g_{t+k} + \mathbf{C}_k \mathbf{A}_0^{-1} \mathbf{\Lambda}_{t+k}^{1/2} \mathbf{P} q_2)' \right) q_1}{q_1' \left(\sum_{k=0}^{K} \mathbf{C}_k \mathbf{\Sigma}_{t+k} \mathbf{C}_k' \right) q_1} = ... \\ =& \frac{\sum_{k=0}^{K} (\mathbf{C}_{1,k} \mathbf{B}_{1,k} g_{t+k} + \mathbf{C}_{1,k} \mathbf{A}_0^{-1} \mathbf{\Lambda}_{t+k}^{1/2} \tau)(\mathbf{C}_{1,k} \mathbf{B}_{1,k} g_{t+k} + \mathbf{C}_{1,k} \mathbf{A}_0^{-1} \mathbf{\Lambda}_{t+k}^{1/2} \tau)'}{\sum_{k=0}^{K} \mathbf{C}_{1,k} \mathbf{\Sigma}_{t+k} \mathbf{C}_{1,k}'}, \end{aligned} \tag{14}$$

where q_1 is a selection vector with 1 in the position $i = 1$ and zeros elsewhere, q_2 is a selection vector with 1 in the position $i = 2$ and zeros elsewhere, and $\mathbf{C}_k$ is the matrix of moving average coefficients measured at each point in time until period k. The combination of selection vectors with the proper column of $\mathbf{P}$ can be written as τ, which is an orthonormal vector that makes $\mathbf{A}_0^{-1} \mathbf{\Lambda}_t^{1/2} \tau$ the impact of a news shock over the variables.

One additional complication that arises is that the share of the forecast error variance of the news shock depends on g_t, $\mathbf{\Lambda}_t^{1/2}$ and $\mathbf{\Sigma}_t$. In other words, the variance decomposition depends on the time t in which it is measured. The news shock is identified by picking τ that maximizes the share described in equation 14, but the dependence of this share on t can lead to a different τ in each point in time. This characteristic forms the basis of the identification procedure for the news shock proposed here. The news shock is identified

by solving the optimization problem

$$\tau_t^{news} = argmax \sum_{k=0}^{K} \Gamma_{1,2}(k)_{t,news}, \tag{15}$$

subject to

$$\begin{aligned} &\mathbf{A}_0(1,j) = 0, \forall j > 1 \\ &\tau_t(1,1) = 0 \\ &\tau_t^{'}\tau_t = 1, \end{aligned} \tag{16}$$

where K is an truncation period, and the restrictions imposed imply that the news shock does not have an effect on impact ($t = 0$) and that the τ_t vector is orthonormal.

In practice, two elements introduce additional nonlinearity to the forecast error described in equation 13: the contemporaneous feedback effect that the uncertainty factors g_t have on the variables y_t (because of the stochastic volatility in mean), and the dependence of the time-varying volatility $\mathbf{\Lambda}_t^{1/2}$ on the uncertainty factors g_t. I deal with this nonlinearity by employing a generalized impulse response structure[10] in substitution for the forecast error described by equation 13. Since generalized impulse response structures do not depend on the model functional form, this substitution makes the procedure even more broad by allowing the identification of news shocks under different forms of nonlinear and time-varying relationships.

The generalized impulse responses are constructed by creating simulated shocked and baseline paths. The difference between these two paths captures the effect of the desired shock, conditional on a random simulated innovation $\omega_{j,t}$, where j identifies the variable. The overall effect of the identified shock is the average of the difference between the baseline and shocked paths across a significant number of random innovations $\omega_{j,t}^r$.

The full identification procedure and steps for the generalized impulse responses are described in Appendix F. To summarize, it is possible to show that, conditional on the draw r of the random innovation $\omega_{j,t}^r$, on the information set containing all the known

[10] Adapting the procedure proposed by Koop, Pesaran, and Potter (1996) and Pesaran and Shin (1998).

history up to time t defined as $\mathbf{Z}_t = (y_{t-p}, ..., y_t; g_{t-p}, ..., g_t)$,[11] and on the coefficient matrices $\mathbf{\Pi} = [\mathbf{A}_i, \mathbf{B}_i, \mathbf{D}_i, \beta_j, \gamma_j, \delta]$, the generalized impulse response at time k of a generic utilization-adjusted TFP shock is given by

$$\begin{aligned} GI^r_{TFP,t}(k, \tau^r_{TFP}, \omega^r_{j,t}, \mathbf{Z}_t, \mathbf{\Pi}) = \mathbb{E}[y^r_{t+k,TFP}, g^r_{t+k,TFP} | \tau^r_{TFP}, \mathbf{\Lambda}^r_{t+k,TFP}, \omega^r_{j,t}, \mathbf{Z}_t, \mathbf{\Pi}] \\ - \mathbb{E}[y^r_{t+k,base}, g^r_{t+k,base} | \mathbf{\Lambda}^r_{t+k,base}, \omega^r_{j,t}, \mathbf{Z}_t, \mathbf{\Pi}], \end{aligned} \tag{17}$$

where τ^r_{TFP} is a vector with 1 in the first position (where utilization-adjusted TFP is ordered first in the VAR) and zeros elsewhere.

With this setup, it is possible to substitute the TFP impulse responses ($\mathbf{C}_{1,k}\mathbf{B}_{1,k}g_{t+k} + \mathbf{C}_{1,k}\mathbf{A}_0^{-1}\mathbf{\Lambda}^{1/2}_{t+k}\tau$) in equation 14 for $GI^r_{TFP,t}(k, \tau^r_{TFP}, \omega^r_{j,t}, \mathbf{Z}_t, , \mathbf{\Pi})$, or simply $GI^r_{TFP,t}(k)$ for notation purposes.

A news shock for a draw r of the random innovation $\omega^r_{j,t}$ can be identified in each period t as

$$\tau^r_{t,news} = \arg\max \frac{\sum_{k=0}^{K} GI^r_{TFP,t}(k, \tau) GI^r_{TFP,t}(k, \tau)'}{\sum_{k=0}^{K} \mathbf{C}_1 \mathbf{\Sigma}_{t+k} \mathbf{C}_1'}, \tag{18}$$

subject to

$$\begin{aligned} &\mathbf{A}_0^{-1}(1, j) = 0, \quad \forall j > 1, \\ &\tau(1, 1) = 0, \\ &\tau'\tau = 1. \end{aligned} \tag{19}$$

After obtaining the identification vector for the news shock $\tau^r_{t,news}$ for the draw r of the random innovations $\omega^r_{j,t}$, it is possible to construct the generalized impulse responses for the news shock at each point in time. Conditional on the draw r of the random innovation $\omega^r_{j,t}$, on the information set $\mathbf{Z}_t$, and on the coefficients $\mathbf{\Pi}$, the generalized impulse response at time k of the technology news shock is given by

$$\begin{aligned} GI^r_{t,news}(k, \tau^r_{t,news}, \omega^r_{j,t}, \mathbf{Z}_t, \mathbf{\Pi}) = \mathbb{E}[y^r_{t+k,news}, g^r_{t+k,news} | \tau^r_{t,news}, \mathbf{\Lambda}^r_{t+k,news}, \omega^r_{j,t}, \mathbf{Z}_t, \mathbf{\Pi}] \\ - \mathbb{E}[y^r_{t+k,base}, g^r_{t+k,base} | \mathbf{\Lambda}^r_{t+k,base}, \omega^r_{j,t}, \mathbf{Z}_t, \mathbf{\Pi}]. \end{aligned} \tag{20}$$

[11] Where $g_t = (\ln m_t; \ln f_t)$.

Taking the averages of each path across a sufficiently large number of draws of the random innovations $\omega_{j,t}^{r}$, the overall generalized impulse response at time k of a news shock, conditional on the information set at time t, is given by

$$\begin{aligned} GI_{t,news}(k, \tau_{t,news}, \mathbf{Z}_t, \mathbf{\Pi}) = &[\bar{y}_{t+k,news}(k, \tau_{t,news}, \mathbf{Z}_t, \mathbf{\Pi}), \bar{g}_{t+k,news}(k, \tau_{t,news}, \mathbf{Z}_t, \mathbf{\Pi})] \\ &- [\bar{y}_{t+k,base}(k, \mathbf{Z}_t, \mathbf{\Pi}), \bar{g}_{t+k,base}(k, \mathbf{Z}_t, \mathbf{\Pi})]. \end{aligned} \tag{21}$$

Note that this identification procedure is a generalization of the standard homoskedastic Barsky and Sims (2011) identification. With a time invariant covariance model and no exogenous variables, the Barsky and Sims (2011) procedure can be nested by the structure presented here. Consider, for example, equation 7. If there are no time-varying volatility or exogenous variables, this equation is reduced to

$$y_t = \mathbf{A}(L)y_t + \mathbf{A}_0^{-1}\mathbf{\Lambda}^{1/2}\epsilon_t, \tag{22}$$

and its moving average representation is simply

$$y_t = \mathbf{C}(L)\mathbf{A}_0^{-1}\mathbf{\Lambda}^{1/2}\epsilon_t. \tag{23}$$

Now, considering the same linear mapping between the innovations (ϵ_t) and the structural shocks (s_t) as in equation 9, the share of the forecast error variance of the news shock defined in equation 14 becomes

$$\begin{aligned} \Gamma_{1,2}(k)_{news} = &\frac{q_1' \left(\sum_{k=0}^{K} (\mathbf{C}_k \mathbf{A}_0^{-1} \mathbf{\Lambda}^{1/2} \mathbf{P} q_2)(\mathbf{C}_k \mathbf{A}_0^{-1} \mathbf{\Lambda}^{1/2} \mathbf{P} q_2)' \right) q_1}{q_1' \left(\sum_{k=0}^{K} \mathbf{C}_k \mathbf{\Sigma} \mathbf{C}_k' \right) q_1} = ... \\ = &\frac{\sum_{k=0}^{K} (\mathbf{C}_{1,k} \mathbf{A}_0^{-1} \mathbf{\Lambda}^{1/2} \tau)(\mathbf{C}_{1,k} \mathbf{A}_0^{-1} \mathbf{\Lambda}^{1/2} \tau)'}{\sum_{k=0}^{K} \mathbf{C}_{1,k} \mathbf{\Sigma} \mathbf{C}_{1,k}'} \end{aligned} \tag{24}$$

and $\Gamma_{1,2}(k)_{news}$ does not depend on t anymore. The procedure of finding τ that maximizes the share of the forecast error variance of equation 24 under the same restrictions described in equation 16 is equivalent to the Barsky and Sims (2011) procedure.

3.2 Measuring the uncertainty transmission effect

The nonlinear model proposed here is flexible enough to investigate whether the effects of news about future productivity depend on the level of uncertainty in the economy. First moment shocks can influence (and be influenced by) the level of uncertainty through two nonlinear feedback devices: a contemporaneous feedback of uncertainty to the mean of the variables, and the lagged feedback effect of the variables to uncertainty. These devices allow expectations on macro and financial conditions to be updated based on the arrival of information about future technology developments. If this update is negligible, or is just noise around the news shock effect, the impulse responses of a news shock under this identification should be similar to the traditional covariance-stationary procedure.

I propose here two counterfactuals to evaluate the relation between news shocks and the level of uncertainty. The purpose of the first counterfactual is to check whether the initial uncertainty condition matters for the effect of the news shock, and the second check whether there is a transmission effect of the news shock through uncertainty.

For the first counterfactual, I fix the macroeconomic and financial uncertainties to their means, to verify whether the news shock effects change in comparison to the identification with time-varying uncertainty. The procedure consists of calculating the difference between the generalized impulse responses from the time-varying procedure described by equation 21, and an artificial generalized impulse response in which the initial condition is changed.

Formally, define the artificial information set containing all the known history up to time t and the means of the macro and financial uncertainties as $\mathbf{Z}_t^* = (y_{t-p}, ..., y_t; \overline{g})$, where $\overline{g} = (\frac{1}{T}\sum_{t=1}^{T} \ln m_t; \frac{1}{T}\sum_{t=1}^{T} \ln f_t)$. Following the steps described in section 3.1, the artificial generalized impulse responses with fixed initial uncertainty conditions can be constructed as

$$\begin{aligned} GI^*_{t,news}(k, \tau^*_{t,news}, \mathbf{Z}^*_t, \mathbf{\Pi}) = \mathbb{E}[y_{t+k}, g_{t+k} | \tau^*_{t,news}, \mathbf{\Lambda}^*_{t+k,news}, \mathbf{Z}^*_t, \mathbf{\Pi}] \\ - \mathbb{E}[y_{t+k}, g_{t+k} | \mathbf{\Lambda}^*_{t+k}, \mathbf{Z}^*_t, \mathbf{\Pi}]. \end{aligned} \tag{25}$$

The final effect of the initial uncertainty condition on the news shock can be calculated as the difference between the generalized impulse responses from equation 21 and from equation 25, as in

$$GI_{t,level} = GI_{t,news}(k, \tau_{t,news}, \mathbf{Z}_t, \mathbf{\Pi}) - GI^*_{t,news}(k, \tau^*_{t,news}, \mathbf{Z}^*_t, \mathbf{\Pi}). \tag{26}$$

The second counterfactual aims to check whether there is a nonlinear feedback between uncertainty and the news shock. It involves shutting down the contemporaneous feedback of uncertainty to the mean of the variables, and the lagged feedback effect of the variables to uncertainty. Recalling the Main and Uncertainty VARs (equations 1 and 5), the contemporaneous feedback of uncertainty to the mean of the variables is captured by the coefficients $\mathbf{B}_i$ in equation 1, and the lagged feedback effect of the variables to uncertainty by the coefficients δ in equation 5. Shutting down the nonlinear feedback (to and from) uncertainty means restricting to zero the coefficient matrices $\mathbf{B}_i$ and δ. Following these restrictions, the Main and Uncertainty VARs would be respectively written as

$$y_t = \mathbf{A}_1 y_{t-1} + ... + \mathbf{A}_p y_{t-p} + v_t, \tag{27}$$

and

$$g_t = \mathbf{D}_1 g_{t-1} + ... + \mathbf{D}_k g_{t-k} + u_t. \tag{28}$$

The procedure for the second counterfactual consists of calculating the difference between the generalized impulse responses from the time-varying procedure described by equation 21, and an artificial generalized impulse response in which the coefficients matrices $\mathbf{B}_i$ and δ are restricted to zero. Formally, define a restricted set of coefficients as $\mathbf{\Pi}^\dagger = [\mathbf{A}_i, \mathbf{B}_i = \mathbf{0}, \mathbf{D}_i, \beta_j, \gamma_j, \delta = \mathbf{0}]$. Following the steps described in section 3.1, the artificial generalized impulse responses with no uncertainty feedback can be constructed as

$$\begin{aligned} GI^\dagger_{t,news}(k, \tau^\dagger_{t,news}, \mathbf{Z}_t, \mathbf{\Pi}^\dagger) = \mathbb{E}[y_{t+k}, g_{t+k} | \tau^\dagger_{t,news}, \mathbf{\Lambda}^\dagger_{t+k,news}, \mathbf{Z}_t, \mathbf{\Pi}^\dagger] \\ - \mathbb{E}[y_{t+k}, g_{t+k} | \mathbf{\Lambda}^\dagger_{t+k}, \mathbf{Z}_t, \mathbf{\Pi}^\dagger]. \end{aligned} \tag{29}$$

The final effect of the transmission (to and from) uncertainty on the news shock can be calculated as the difference between the generalized impulse responses from equation 21 and from equation 29, as in

$$GI_{t,feedback} = GI_{t,news}(k, \tau_{t,news}, \mathbf{Z}_t, \mathbf{\Pi}) - GI^{\dagger}_{t,news}(k, \tau^{\dagger}_{t,news}, \mathbf{Z}_t, \mathbf{\Pi}^{\dagger}). \tag{30}$$

3.3 Identification procedure for macroeconomic and financial uncertainty shocks

The uncertainty shocks are modeled as a shock to the common uncertainty factors that compose the volatilities of each variable. Since these factors are also included in the Main VAR, the uncertainty shock can affect both the mean and the variance of the variables of interest y_t.

In this model, there are two uncertainty factors (macro and financial), which share a full variance-covariance matrix defined as

$$\mathbf{\Phi}_u = \begin{bmatrix} \phi_{n+1} & \phi_{n+3} \\ \phi_{n+3} & \phi_{n+2} \end{bmatrix}. \tag{31}$$

This setup demands imposing an orthogonalization structure to achieve the structural macro and financial shocks. Employing a Cholesky structure leads to two possible orthogonalizations: macro uncertainty ordered first with financial uncertainty ordered last, and the inverse.

As a benchmark, I define financial variables as "fast" variables, while macro variables are "slow" variables. It means that financial uncertainty can react contemporaneously to macroeconomic uncertainty shocks, but macroeconomic uncertainty can only react to financial uncertainty shocks with one lag. This ordering is equivalent to modeling macro uncertainty first and financial uncertainty last in the Cholesky identification structure.

In contrast to the news shock, the variance-covariance matrix of the uncertainties does not change across time. I identify both shocks at the last observation T, so the

information set here is $\mathbf{Z}_T = (y_{T-p}, ..., y_T; g_{T-p}, ..., g_T)$.[12]

The full identification procedure is described in Appendix F, but the general idea is to produce a baseline and a shocked path for y_t, g_t and $\mathbf{\Lambda}_t$ based on each of the uncertainty shocks (macro and financial). The shocks are identified as

$$\begin{aligned} \tau^r_{macro} &= \tilde{\mathbf{\Phi}}_u * q_i^{macro}, \\ \tau^r_{fin} &= \tilde{\mathbf{\Phi}}_u * q_i^{fin}, \end{aligned} \tag{32}$$

where $\tilde{\mathbf{\Phi}}_u$ is the lower triangular Cholesky decomposition of $\mathbf{\Phi}_u$, r is the index of the set of randomly drawn $\omega^r_{j,t}$ innovations, q_i^{macro} is a 2×1 vector with 1 in the first position and zero in the second, and q_i^{fin} is a 2×1 vector with zero in the first position and 1 in the second. For $T+1$, I construct a one standard deviation shock on macro uncertainty by substituting $(u_{m,t}, u_{f,t})'$ in equation D.6 for τ^r_{macro}. I then construct by simulation a macro shocked path from $T+1$ to $T+K$ for $y^r_{t,macro}$, $g^r_{t,macro}$ and $\mathbf{\Lambda}^r_{t,macro}$ using equation D.6. I repeat the process for the financial uncertainty by using τ^r_{fin} to construct paths for $y^r_{t,fin}$, $g^r_{t,fin}$ and $\mathbf{\Lambda}^r_{t,fin}$.

By employing the generalized impulse response structure described in Appendix F, the final economic effect of the uncertainty shock is measured as

$$\begin{aligned} GI_{macro}(k, \tau_{macro}, \mathbf{Z}_T, \mathbf{\Pi}) &= \mathbb{E}[y_{T+k}, g_{T+k} | \tau_{macro}, \mathbf{\Lambda}_{T+k,macro}, \mathbf{Z}_T, \mathbf{\Pi}] \\ &\quad - \mathbb{E}[y_{T+k}, g_{T+k} | \mathbf{\Lambda}_{T+k}, \mathbf{Z}_T, \mathbf{\Pi}], \\ GI_{fin}(k, \tau_{fin}, \mathbf{Z}_T, \mathbf{\Pi}) &= \mathbb{E}[y_{T+k}, g_{T+k} | \tau_{fin}, \mathbf{\Lambda}_{T+k,fin}, \mathbf{Z}_T, \mathbf{\Pi}] \\ &\quad - \mathbb{E}[y_{T+k}, g_{T+k} | \mathbf{\Lambda}_{T+k}, \mathbf{Z}_T, \mathbf{\Pi}]. \end{aligned} \tag{33}$$

4 Latent uncertainty measures

In this Section I present the estimated macro and financial uncertainties from the stochastic volatility in mean model presented in Section 2. The (estimated) stochastic volatility of each variable is composed of a common factor, which can be macroeconomic or financial depending on the underlying variable, and an idiosyncratic component. The common fac-

[12] Where $g_T = (\ln m_T; \ln f_T)$.

tors across the volatilities are the estimations of aggregate macroeconomic and financial uncertainties.

Figure 3 displays the estimated aggregate macroeconomic uncertainty, and Figure 4 shows the estimated financial uncertainty. The stochastic volatilities of the macroeconomic and financial variables are presented in Appendix H. The economic assumption that macro and financial uncertainty may be related to each other is captured by the interaction between the two uncertainty measures included in the Uncertainty VAR (equation 5) and the full variance-covariance matrix between the two factors (equation 6). Figures 3 and 4 show that some periods in time share high macro and financial uncertainties, but some are marked by either a hike mainly in macro or financial uncertainty. Comparing these series with the recessions identified by the National Bureau of Economic Research (NBER), it is possible to match each recession with a macroeconomic uncertainty hike, a financial uncertainty hike, or both.

Figure 3 Aggregate macroeconomic uncertainty

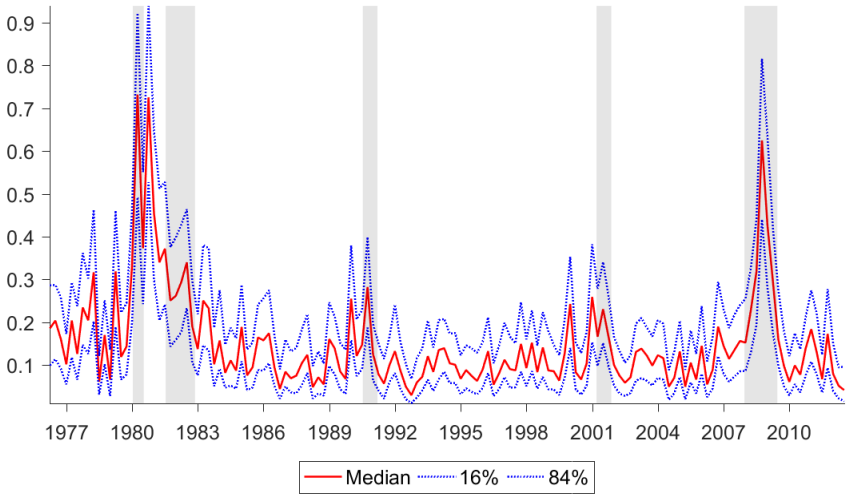

Note: Macroeconomic uncertainty measured as the common factor on macroeconomic volatilities. The dotted lines define the 68% confidence bands computed with 200 posterior draws. The VAR model includes all variables in Tables G.1 and G.2. Shaded areas are the recession periods calculated by the NBER.

The Great Moderation period (mid-1980s) for example, characterized by a decline in the business cycle volatility of aggregate macroeconomic variables, is captured by a hike in the macroeconomic uncertainty. During the dot-com crisis (1999-2001), which

Figure 4 Aggregate financial uncertainty

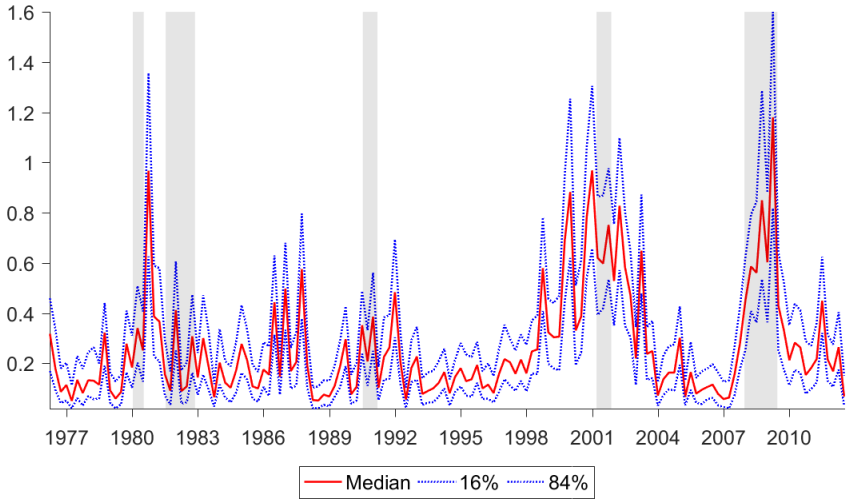

Note: Financial uncertainty measured as the common factor on financial volatilities. The dotted lines define the 68% confidence bands computed with 200 posterior draws. The VAR model includes all variables in Tables G.1 and G.2. Shaded areas are the recession periods calculated by the NBER.

was mainly a speculative financial bubble in the stock market, there is a higher financial uncertainty. The 2008 crisis shows high macro and financial uncertainties.

While the uncertainty measures match crisis periods, they also follow closely the monthly macro and financial uncertainties estimated by Ludvigson et al. (2016), which I take here as a benchmark for comparison purposes. The macroeconomic uncertainty presented in Figure 3 and the 1-month ahead macroeconomic uncertainty from Ludvigson et al. (2016) share a correlation of 0.76 over the period 1975Q1 and 2012Q3,[13] with 0.77 for both the 3-months ahead and 12-months ahead versions. The correlation of the financial uncertainty presented in Figure 4 and the 1-month ahead financial uncertainty from Ludvigson et al. (2016) is 0.68, with same coefficient when taking into consideration the 3-months or 12-months ahead versions of the financial uncertainty.

The two series estimated here are also correlated with each other, a direct result of the possibility of transmission of macro-to-financial uncertainty, and vice versa. The correlation coefficient of the two series is 0.36. The uncertainty measures from Ludvigson

[13]I transform the uncertainty measures calculated by Ludvigson et al. (2016) from monthly to quarterly by averaging across the quarter.

et al. (2016) present a higher correlation with each other. Considering the 1-month ahead macro and financial uncertainty, the correlation coefficient is 0.53 over the period 1975Q1 and 2012Q3. The correlation coefficients of the 3-months and 12-months ahead uncertainty versions are, respectively, 0.52 and 0.45.

It is important to notice that the estimation procedure for the measures presented here is substantially different from the Ludvigson et al. (2016) methodology. First, Ludvigson et al. (2016) use of the FRED-MD database[14] with stationary monthly data, while I use quarterly data in levels. Second, Ludvigson et al. (2016) construct uncertainty measures by averaging the conditional volatility of unforecastable components of the future value of the macroeconomic or financial series. Here, I estimate the uncertainty measures with a particle filter, where these uncertainties depend on the (lagged) dependent variables, and the dependent variables can react contemporaneously to the uncertainties (stochastic volatility in mean). Lastly, Ludvigson et al. (2016) and this paper use different variables. While Ludvigson et al. (2016) employ 132 macro series and 147 financial series,[15] I construct the uncertainty measures using only 14 macro and 14 financial series.

5 Time-varying Impulse responses to a news shock

In this Section I present the results of the news shock identification. For every point in time the news shock economic responses are different, conditional on the estimated time-varying volatility. This procedure makes it possible to understand the different effects of a news shock on periods of high and low macro and financial uncertainty.

Figures 5 and 6 present the economic responses of selected variables after a news shock, identified and calculated for each point in time as generalized impulse responses.[16] The graphs in Figure 5 show impulse responses in three dimensions: period in time of identification (x-axis), size of impact (y-axis) and the effect h quarters ahead (each line). Figure 6 presents these same impulse responses "sliced" at selected forecast horizons.

[14] McCracken and Ng (2015).

[15] Please refer to the On-line Appendix of Jurado et al. (2015) for a detailed description of the database employed by the authors.

[16] As described in Appendix F. The generalized impulse responses for all the variables included in the VAR can be found in Appendix J.

Figure 5 Time-varying effects of news shocks

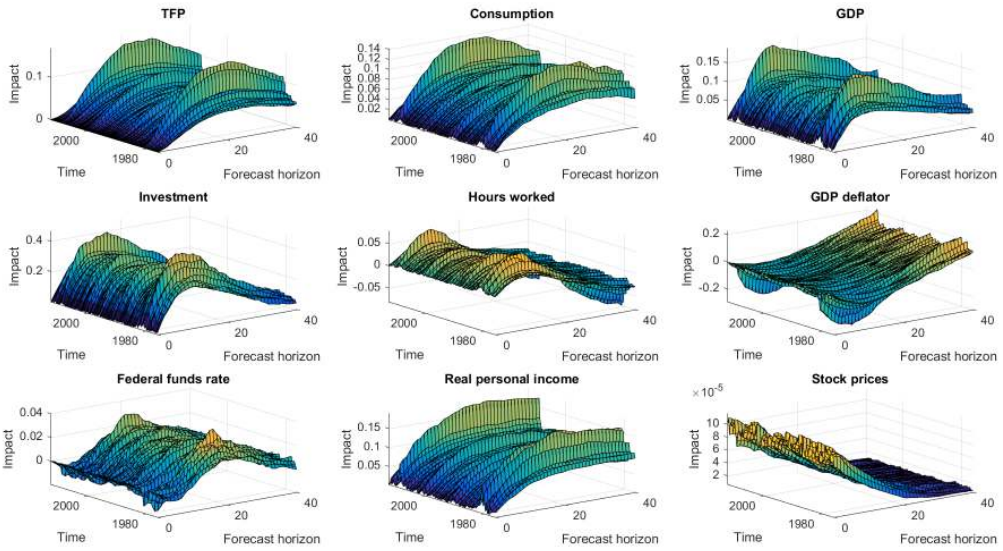

Note: The news shock is identified for each period in time under the procedure proposed in Section 3.1. The generalized impulse responses for each period are the average of 1,000 simulated random innovations, as described in Appendix F.

Figure 6 Time-varying effects of news shocks over different forecast horizons

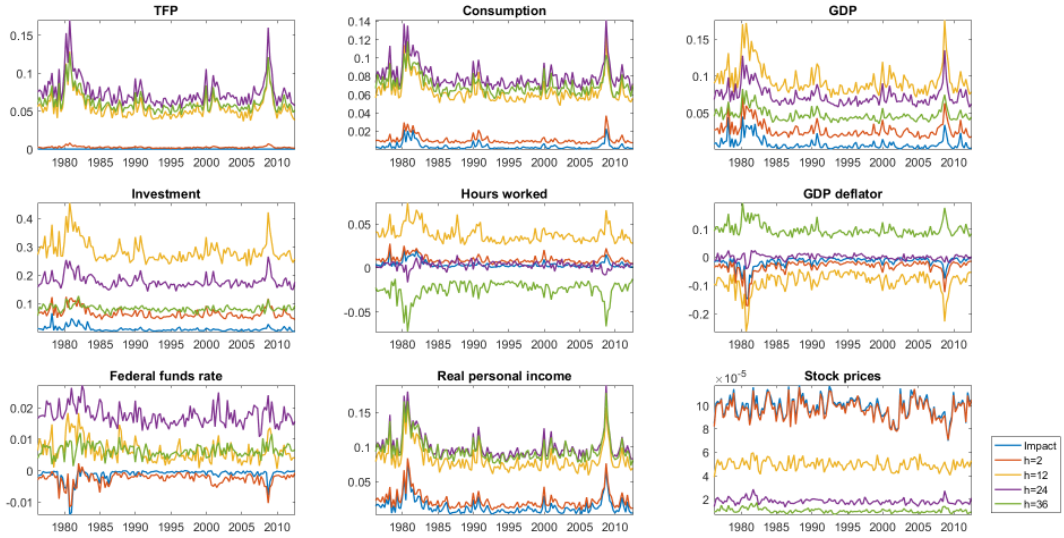

Note: The news shock is identified for each period in time under the procedure proposed in Section 3.1. The generalized impulse responses for each period are the average of 1,000 simulated random innovations, as described in Appendix F. Each line corresponds to the effect of the news shock h-quarters ahead from the point in time, as "slices" of the graphs from Figure 5.

The top-left graph of Figure 6 shows the effect of a technology news shock over the utilization-adjusted TFP. The identification procedure of the news shock maximizes the

variance decomposition of this variable over a fixed forecast horizon of 40 quarters ahead, imposing a zero effect on impact ($h = 0$). This graph provides evidence for how different the effects of a news shock can be over time when a time-varying volatility is taken into account. The long-term effect of a news shock identified in the period 1980-1983 or during the 2008 crisis is about twice the effect in more stable periods, as for example, the early 1990s.

These differences over time are also found in the impulse responses for consumption, GDP, investment and real personal income. The positive effect of a news shock on consumption and personal income peaks after about 12 quarters. This new higher level of consumption and real personal income is sustained in the long-term, while GDP and investment peak at about 12 quarters and decay in the long-term. Nevertheless, the positive effects on consumption, personal income, GDP and investment are more intense during periods in which the effect of a news shock on utilization-adjusted TFP is stronger.

The responses of hours worked are positive in the medium-term ($h = 12$), and negative in the long-term ($h = 36$). These effects are substantially more intense in periods of higher volatility (early 1980s and 2008). There is a deflationary effect in the medium-term after a news shock, as evidenced by the literature.[17] By employing a covariance-stationary identification procedure, Barsky et al. (2014) point out that the peak of the negative effect on inflation is about 10 quarters after the news shock. Figure 6 shows that, after 12 quarters, there is indeed a deflationary effect, but this is much more intense in periods of high volatility.

The effect on stock prices is positive, as initially indicated by Beaudry and Portier (2006). These effects peak on impact ($h = 0$) and converge to zero in the long-term. It is worth noting, however, that the effect on stock prices is largely unrelated to the size of the effect of the news shock on utilization-adjusted TFP. The positive news about future technology is interpreted by the stock market in similar way across time, with positive effects on impact.

[17] See, for example, Christiano, Ilut, Motto, and Rostagno (2010), Barsky and Sims (2011) and Barsky, Basu, and Lee (2014).

5.1 News shocks and the relationship to uncertainty

As shown, the effects of a news shock are substantially different across time. In this Section I investigate if these differences come from a potential connection between technology news shocks and uncertainty.

Bloom (2009) shows that uncertainty[18] creates an 'inaction zone' in investment, due to firms becoming more cautious. With firms close to the investment threshold, small positive volatility shocks generate an investment response, while small negative shocks generate no response. The idea is that, after the initial recessive effect of uncertainty, firms would want to scale up their investment plans to address pent-up demand. The result is a medium-term overshoot in productivity growth. Periods of high uncertainty are also related to a higher potential return on investment, increasing the range of growth options (Segal, Shaliastovich, and Yaron, 2015).

Cascaldi-Garcia and Galvao (2017) suggest that uncertainty shocks generate two effects on total factor productivity: a short-term negative reduction on utilization factors, and a medium-term positive effect on the utilization-adjusted productivity. This medium-term positive effect relates to the overshoot in productivity growth idea presented by Bloom (2009). It follows that uncertainty foresees future technology improvements, as a 'good uncertainty' effect. From this literature, one would expect a positive relationship between high uncertainty periods and the positive economic outcomes from a higher expected future technology growth, as in a news shock.

I first evaluate this proposition by calculating the correlation between a series of uncertainty measures and the medium ($h = 12$) and long-term ($h = 36$) effects of a news shock on utilization-adjusted TFP, consumption and GDP. Table 1 presents these correlations, while the description and availability of the uncertainty measures can be found in Table G.3 in Appendix G.

Table 1 shows that the responses to a news shock are (positively) correlated with both macro and financial uncertainties. Generally speaking, the correlation is higher with macroeconomic uncertainty measures, and is higher in the medium-term than in the

[18]Bloom (2009) defines uncertainty as an increase in the volatility of total factor productivity shocks that have a temporary negative effect on output growth.

Table 1 Correlations between news shock economic responses and uncertainty measures

	Medium-term					
	TFP		Consumption		GDP	
Macro uncertainty measures						
Macro uncertainty	0.96	[0.000]	0.92	[0.000]	0.93	[0.000]
LMN-macro-1	0.79	[0.000]	0.73	[0.000]	0.76	[0.000]
LMN-macro-3	0.80	[0.000]	0.74	[0.000]	0.77	[0.000]
LMN-macro-12	0.80	[0.000]	0.74	[0.000]	0.78	[0.000]
Policy uncertainty	0.01	[0.949]	-0.02	[0.772]	0.02	[0.860]
Business uncertainty	-0.01	[0.936]	-0.02	[0.791]	-0.08	[0.373]
SPF disagreement	0.53	[0.000]	0.50	[0.000]	0.55	[0.000]
Financial uncertainty measures						
Financial uncertainty	0.52	[0.000]	0.27	[0.000]	0.39	[0.000]
LMN-fin-1	0.45	[0.000]	0.32	[0.000]	0.39	[0.000]
LMN-fin-3	0.45	[0.000]	0.31	[0.000]	0.39	[0.000]
LMN-fin-12	0.45	[0.000]	0.30	[0.000]	0.39	[0.000]
Realized volatility	0.47	[0.000]	0.39	[0.000]	0.43	[0.000]
VXO	0.65	[0.000]	0.49	[0.000]	0.64	[0.000]

	Long-term					
	TFP		Consumption		GDP	
Macro uncertainty measures						
Macro uncertainty	0.95	[0.000]	0.87	[0.000]	0.85	[0.000]
LMN-macro-1	0.76	[0.000]	0.67	[0.000]	0.67	[0.000]
LMN-macro-3	0.77	[0.000]	0.68	[0.000]	0.68	[0.000]
LMN-macro-12	0.76	[0.000]	0.69	[0.000]	0.68	[0.000]
Policy uncertainty	0.00	[0.973]	-0.03	[0.750]	0.03	[0.757]
Business uncertainty	-0.02	[0.831]	-0.10	[0.231]	-0.08	[0.355]
SPF disagreement	0.51	[0.000]	0.48	[0.000]	0.46	[0.000]
Financial uncertainty measures						
Financial uncertainty	0.45	[0.000]	0.28	[0.000]	0.27	[0.001]
LMN-fin-1	0.41	[0.000]	0.29	[0.000]	0.28	[0.001]
LMN-fin-3	0.40	[0.000]	0.29	[0.000]	0.28	[0.001]
LMN-fin-12	0.40	[0.000]	0.29	[0.000]	0.26	[0.001]
Realized volatility	0.44	[0.000]	0.34	[0.000]	0.35	[0.000]
VXO	0.60	[0.000]	0.52	[0.000]	0.48	[0.000]

Note: The Macro uncertainty and Financial uncertainty in ***bold*** *are the measures calculated in this paper, and presented in Figures 3 and 4. Medium-term and long-term responses are calculated 12 and 40 quarters ahead, respectively. The p-values for the test with zero correlation under the null hypothesis are in brackets. The statistic is calculated as* $t = \rho_0 \sqrt{\frac{T-2}{1-\rho_0^2}}$. *For details on the uncertainty measures and availability, see Table G.3 in Appendix G.*

long-term. There is a high correlation with the aggregated macroeconomic uncertainty estimated here and with the macro uncertainties from Ludvigson et al. (2016).[19] The correlation is also positive and significant with the disagreement measure from the Survey of Professional Forecasters (SPF), ranging from 0.50 to 0.55 in the medium-term, and from 0.46 to 0.51 in the long-term. There is no correlation of the responses with the policy uncertainty calculated by Baker, Bloom, and Davis (2016) and with the business uncertainty from Bachmann, Elstner, and Sims (2013). Although smaller, all the correlations between financial uncertainties and the effects on utilization-adjusted TFP, consumption and GDP are statistically significant.

It is important to note that the news shocks identified across time are normalized, with the same size. The high correlation of the medium and long-term effects presented in Table 1 is a result of the transmission mechanism of the uncertainty measures to the mean of the variables presented in equations 1 and 5. This transmission mechanism makes the news shock stronger in periods of higher macroeconomic and financial uncertainty, as suggested by the data when viewed through the stochastic volatility in mean VAR model.

Figure 7 presents a clearer image of the differences between the effects of a news shock during high and low macroeconomic uncertainty periods. The red lines correspond to the average of generalized impulse responses on periods of high uncertainty, while the blue lines correspond to the average of generalized impulse responses on periods of low uncertainty. I define high uncertainty as the periods with the highest 10% of values for macroeconomic uncertainty, and low uncertainty with the lowest 10% of values.

In the high uncertainty period, the positive effects of a news shock on utilization-adjusted TFP, consumption, investment and real personal income are substantially higher. The path of utilization-adjusted TFP (top-left graph of Figure 7) is flatter in the low uncertainty period, while it has a positive peak about 20 quarters ahead in the high uncertainty period. Cascaldi-Garcia and Galvao (2017) show that, after an uncertainty shock, utilization-adjusted TFP rises in the medium-term, converging to zero in the long-term. This hump-shaped path of utilization-adjusted TFP observed in the high uncertainty

[19]Between 0.78 and 0.96 in the medium-term across TFP, consumption and GDP, and between 0.68 and 0.95 in the long-term.

Figure 7 Impulse responses to news shocks in periods of high and low macro uncertainty

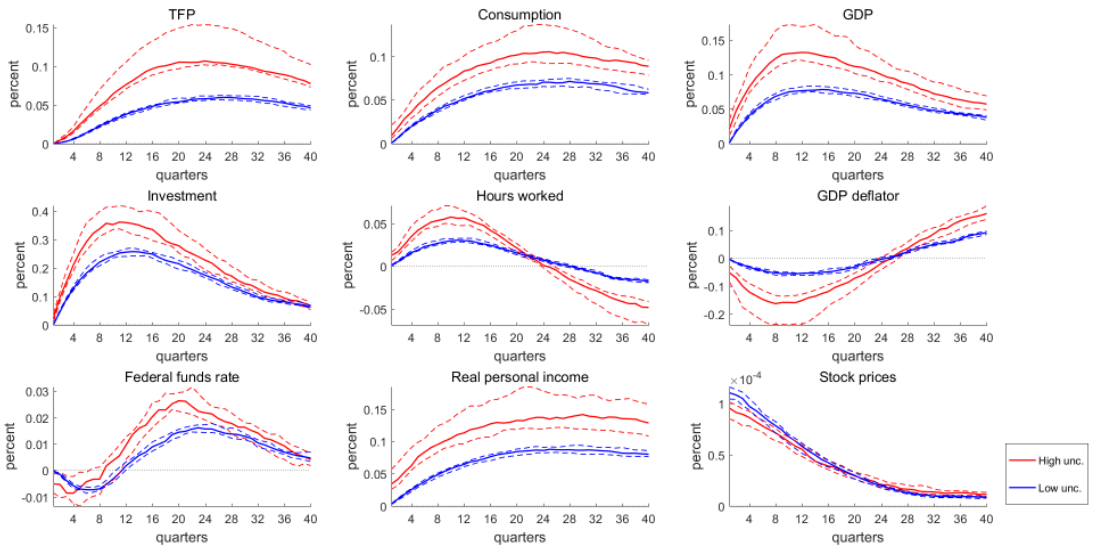

Note: The news shock is identified for each period in time under the procedure proposed in Section 3.1. Red and blue lines correspond to the average of generalized impulse responses on periods of high and low uncertainty, respectively. High and low uncertainty are the periods with the higher and lower 10% values for the macroeconomic uncertainty, respectively. Each impulse response is evaluated at the posterior mean. Dashed lines correspond to 68% distribution of the impulse responses in the high and low periods.

period is in line with the view that uncertainty predicts a medium-term positive effect on technology.

The positive effect on consumption is higher in the high macroeconomic uncertainty period over the entire forecast horizon of 40 quarters, following same pattern as real personal income. With respect to GDP, the biggest difference between the high and low uncertainty periods is in the medium-term. This divergence is a direct result of the economic response of investment, which peaks about two to three years after the news shock occurred. In the long-term, the path of investment in the high uncertainty period converges to the path of the low uncertainty period.

The deflationary effect of the news shock is more pronounced in the high macroeconomic uncertainty period. In the low uncertainty period the response of the GDP deflator is flatter, and close to zero. The effect of the news shock on the hours worked is positive in the medium-term and negative in the long-term under the high uncertainty period, while it is closer to zero under the low uncertainty period. There is no perceptible difference

between the responses of the stock prices in the high or low uncertainty macroeconomic periods. It is positive on impact, converging to zero in the long-term in both cases.

In summary, these results provide evidence that news shocks have quantitatively different effects in periods of high and low uncertainty. In periods of high uncertainty the positive effects of news shocks are boosted, in line with the notion of a transmission mechanism of technology news through uncertainty.

5.2 The uncertainty transmission mechanism of news shocks

How important is uncertainty for the effect of news shocks on the economy? Does it depend only on the level of uncertainty at the time of the shock, or is there an uncertainty transmission mechanism that influences the effect of a news shock throughout time? I investigate these questions by providing two counterfactuals: what would happen to a news shock (i) if uncertainty would remain unchanged across time, or (ii) if there was no feedback effect from uncertainty. Section 3.2 provides the full description of the procedure for these two counterfactuals.

The first counterfactual checks if the initial uncertainty condition matters for the effect of the news shock. Figure 8 presents the impulse responses of a news shock identified with a fixed uncertainty. Differently from Figure 6, the effects of the news shock do not change over time when the initial uncertainty condition is fixed. Figure 9 outlines the importance of the initial uncertainty condition, by showing the differences between the impulse responses with time-varying uncertainty and with fixed uncertainty. This is constructed by taking the responses from Figure 6 and subtracting the responses from Figure 8. The effects of a news shock are more substantial in periods of high uncertainty, confirming the level effect that the initial uncertainty condition generates in the responses to a news shock.

The second counterfactual checks if there is nonlinear feedback between uncertainty and the news shock. Figure 10 presents the generalized impulse responses of a news shock without feedback effect from uncertainty. The pattern of these responses is quite similar to the responses from the full model, in which there is a feedback effect from

Figure 8 Time-varying effects of news shocks over different forecast horizons with fixed uncertainty

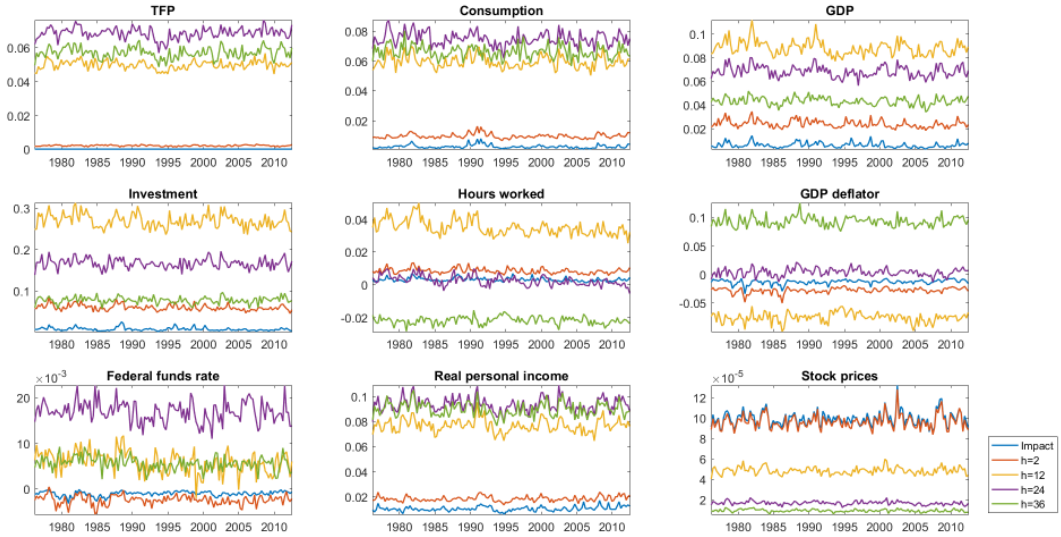

Note: The news shock is identified for each period in time under the procedure proposed in Section 3.2. The generalized impulse responses for each period are the average of 1,000 simulated random innovations, as described in Appendix F. Each line corresponds to the effect of the news shock h-quarters ahead from the point in time.

Figure 9 Differences between responses to a news shock computed with time-varying uncertainty and with fixed uncertainty

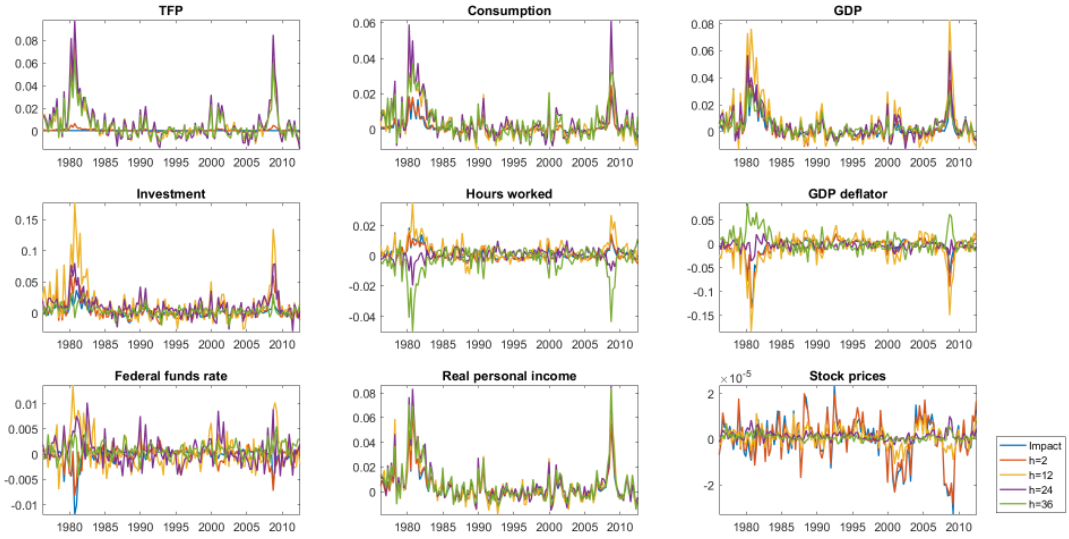

Note: The news shock is identified for each period in time under the procedure proposed in Section 3.2. The generalized impulse responses for each period are the average of 1,000 simulated random innovations, as described in Appendix F. Each line corresponds to the effect of the news shock h-quarters ahead from the point in time.

uncertainty (Figure 6). However, these effects differ in magnitude. Figure 11 depicts the differences between the impulse responses with and without feedback from uncertainty. This is constructed by taking the responses of Figure 6 and subtracting the responses from Figure 10.

Figure 10 Time-varying effects of news shocks over different forecast horizons with no feedback effect from uncertainty

Note: The news shock is identified for each period in time under the procedure proposed in Section 3.2. The generalized impulse responses for each period are the average of 1,000 simulated random innovations, as described in Appendix F. Each line corresponds to the effect of the news shock h-quarters ahead from the point in time.

Overall, the presence of an uncertainty feedback creates a positive bias in the effect of a news shock on consumption, GDP and investment. This can be easily observed by averaging these time-varying impulse responses, as in Figure 12. This Figure summarizes the nonlinear feedback effect of uncertainty over the news shock. On average, the feedback effect generates a positive medium-term effect on utilization-adjusted TFP, investment and GDP. Interestingly, the positive bias on investment peaks after about 10 quarters, a period in which there is still no positive bias on utilization-adjusted TFP. This is evidence that investment is anticipating future expected productivity, in line with the findings of Beaudry and Portier (2006). In the long-term, this positive bias on utilization-adjusted TFP, investment and GDP tends to die out. With regard to consumption and real personal income, there is a positive bias that tends to persist in the long-term.

Figure 11 Differences between responses to a news shock computed with and without feedback effect from uncertainty

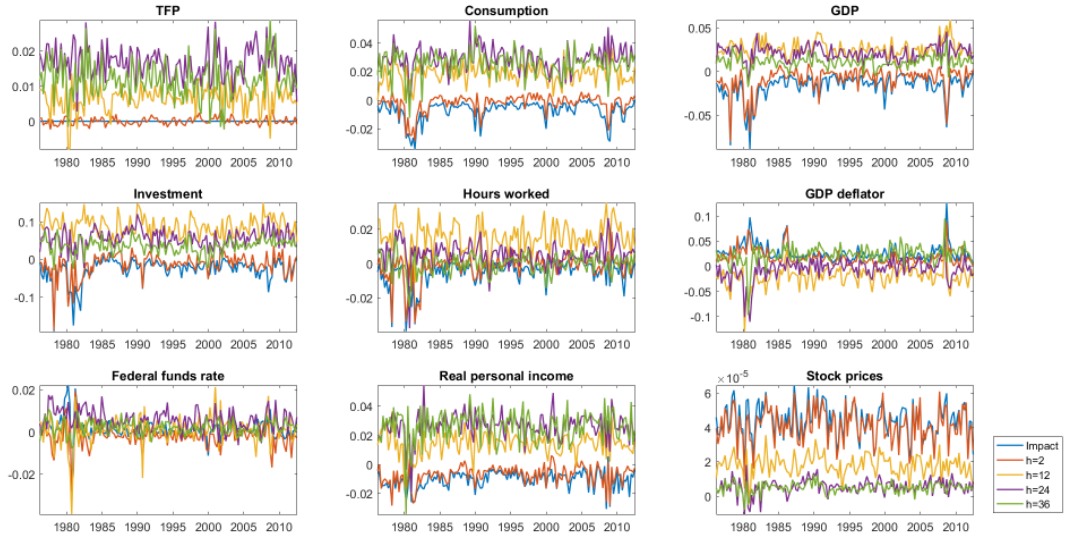

Note: The news shock is identified for each period in time under the procedure proposed in Section 3.2. The generalized impulse responses for each period are the average of 1,000 simulated random innovations, as described in Appendix F. Each line corresponds to the effect of the news shock h-quarters ahead from the point in time.

Figure 12 Percentiles of the differences between responses to a news shock computed with and without feedback effect from uncertainty

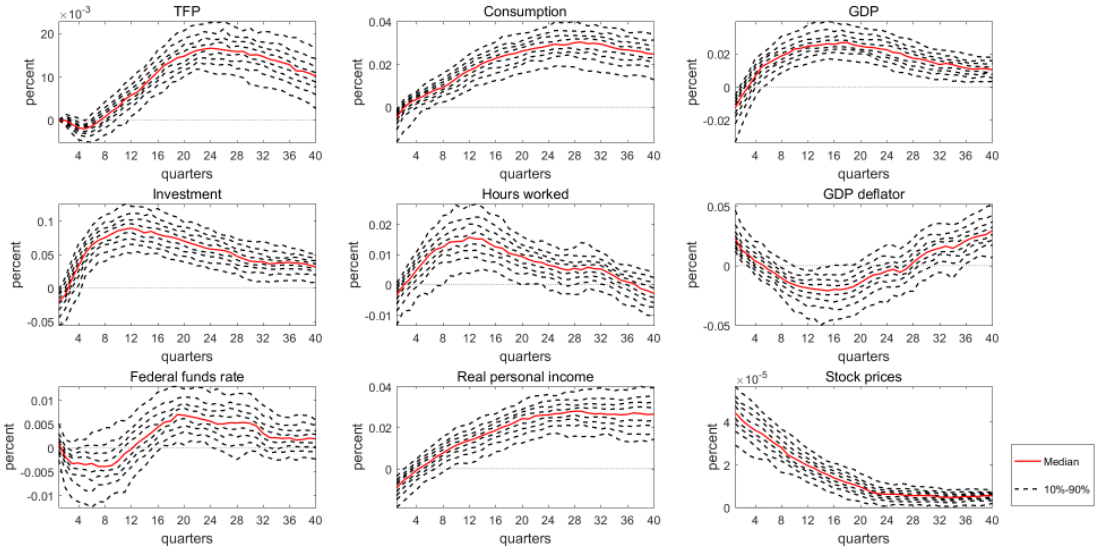

Note: The news shock is identified for each period in time under the procedure proposed in Section 3.2. Each line corresponds to the deciles of the differences between the news shock impulse responses with and without feedback effect from uncertainty, identified in each point in time and calculated at the posterior mean. The red line is the median.

In summary, the counterfactuals presented here indicate that uncertainty and news shocks are linked through two mechanisms: an initial condition effect and a transmission effect. The initial condition effect means that, if the initial level of uncertainty in the economy is high, the effects of the news shock will also be high. This evidence is in line with the 'good uncertainty' shock literature, described before.

The transmission effect is more complex. The empirical results from the second counterfactual show that when macro and financial uncertainties are allowed to react to news shocks, the positive effects of such news are amplified. These results are in line with a new stream in the literature on news and uncertainty shocks, which explores the dynamics of uncertainty updating based on the arrival of news. Forni, Gambetti, and Sala (2017) propose a model in which uncertainty is generated by news about future developments in economic conditions. Uncertainty arises from the fact that these conditions are not perfectly predicted by the economic agents. Berger, Dew-Becker, and Giglio (2017) define an uncertainty shock as a second-moment news, or changes in the expected future volatility of aggregate stock returns. The authors argue that news about the squared growth rates are changes in the conditional variance, which is equivalent to an uncertainty shock.

In summary, the results from the second counterfactual suggest that the arrival of information about future technology makes the economic agents update not only their expectations about future productivity, as in the news shock literature, but also their expectations about macroeconomic and financial conditions, *proxies* to uncertainty. This process is continuous, with consecutive updates as the effects of this new information materialize. More broadly, the level of uncertainty reacts to information about the state of the economy, and the state of the economy reacts to the level of uncertainty.

6 Responses to macroeconomic and financial uncertainty shocks

In this Section I present generalized impulse responses of macroeconomic and financial uncertainty shocks.[20] These responses help to better understand the link between uncertainty and news shocks. The uncertainty shocks are disturbances to the common macroeconomic and uncertainty volatility factors, or a second-moment shock to the variables. The benchmark results presented here consider the macro uncertainty as the first orthogonalization position, and the financial uncertainty as the last.[21]

Figure 13 shows the generalized impulse responses of a financial uncertainty shock for selected variables. The full generalized impulse responses can be found in Appendix J. The most interesting result here is the effect on utilization-adjusted TFP. After the financial uncertainty shock, utilization-adjusted TFP increases in the medium-term, starting from a zero effect on impact ($t = 0$), and converging to zero in the long-term. This path resembles the expected result of a news shock on this variable. This result is in line with Cascaldi-Garcia and Galvao (2017), who show that a financial uncertainty shock foresees a medium-term positive hike in utilization-adjusted TFP.[22]

The similarity of the responses on utilization-adjusted TFP presented here and in Cascaldi-Garcia and Galvao (2017) are noteworthy, in the sense that the identification method for the financial shock is substantially different. While Cascaldi-Garcia and Galvao (2017) identify the financial uncertainty shock as the orthogonalization that maximizes the variance decomposition of an observable *proxy* of financial uncertainty in the short-term, here the financial uncertainty shock is a second moment shock to a latent estimated financial uncertainty measure from a stochastic volatility process. Nevertheless, the impact of financial uncertainty on technology follows the evidence from Cascaldi-Garcia and Galvao (2017).

[20] Appendix F presents the procedure of identification of the macro and financial uncertainty shocks and the calculation of the generalized impulse responses.

[21] The alternative impulse responses considering the inverted ordering (first financial and second macro uncertainty) are presented in Appendix I.

[22] It is also robust to the alternative identification with financial uncertainty ordered first, as presented in Figure I.1 in Appendix I.

Figure 13 Impulse responses to a financial uncertainty shock

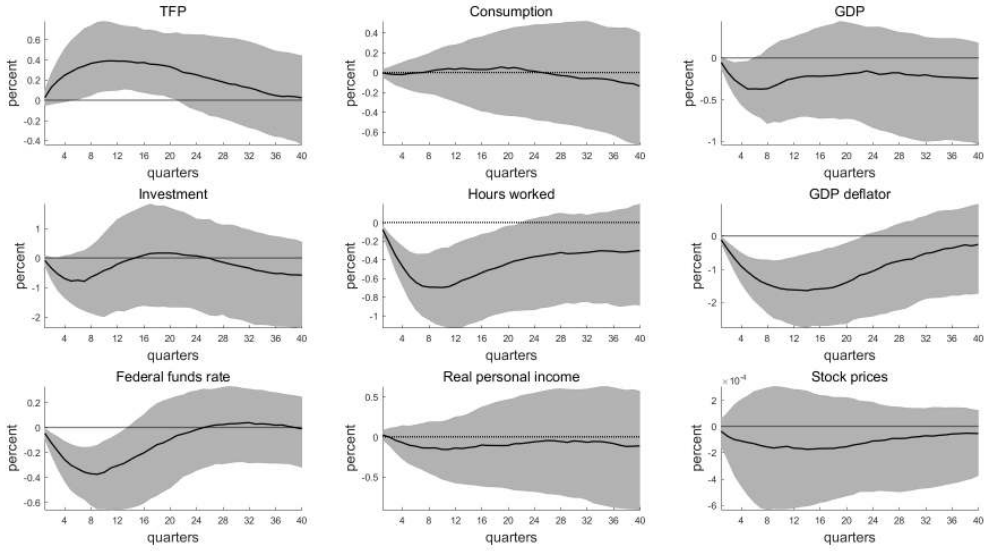

Note: The uncertainty shocks are identified through Cholesky decomposition with macroeconomic uncertainty ordered first, and financial uncertainty ordered last, as described in Section 3.3. The generalized impulse responses of the uncertainty shock are the average of 1,000 simulated random innovations, as described in Appendix F. The shaded areas define the 68% confidence bands computed with 200 posterior draws.

The effect of the financial shock on other variables is distinct from the utilization-adjusted TFP. There is no significant effect on consumption. GDP falls after the shock, driven by a reduction on investment. Both GDP and investment paths converge to zero in the medium-term, confirming the short-lived characteristic of uncertainty shocks. There is a deflationary effect, and the Federal funds rate goes down to counteract the recessionary impact.

Figure 14 presents the generalized impulse responses of a macroeconomic uncertainty shock on selected variables. The full generalized impulse responses can be found in Appendix J. Although smaller, the effect on utilization-adjusted TFP is similar to that observed in the financial uncertainty shock, with a medium-term positive effect.[23] The effect on consumption, GDP and investment are virtually zero. There is a negative impact on hours worked, and a deflationary effect in the medium-term.

[23]Similar results can be found in the alternative identification with financial uncertainty ordered first, as presented in Figure I.2 in Appendix I.

Figure 14 Impulse responses to a macroeconomic uncertainty shock

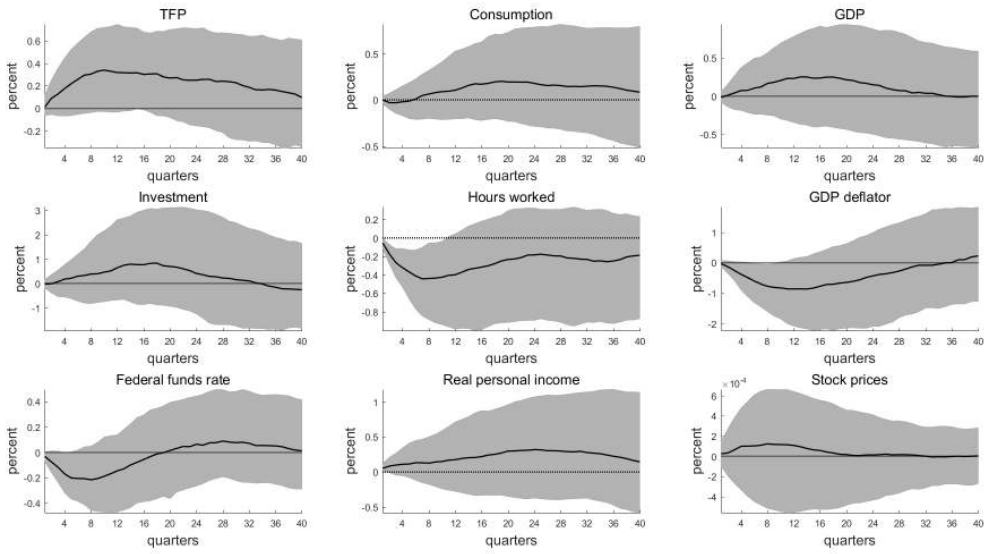

Note: The uncertainty shocks are identified through Cholesky decomposition with macroeconomic uncertainty ordered first, and financial uncertainty ordered last, as described in Section 3.3. The generalized impulse responses of the uncertainty shock are the average of 1,000 simulated random innovations, as described in Appendix F. The shaded areas define the 68% confidence bands computed with 200 posterior draws.

7 Conclusion

This paper shows that the positive economic effects of news on the future increase in technology differ depending on the level of uncertainty of the economy. It contributes to the literature on shocks driven by agents' beliefs in two ways.

First, I propose an innovative method of checking whether the effects of technology news shocks change depending on the point in time at which it is identified. By employing this identification strategy, I show that economic responses to a news shock vary quantitatively across time. While the conventional Barsky and Sims (2011) identification is not robust to changes in the estimation period,[24] the results from this paper indicate that processes with time invariant covariances may not be appropriate for a news shock identification. Moreover, the fact that the responses to news shocks vary significantly over time helps to explain why there is still no consensus in the news shock literature

[24]See an empirical evaluation in the Introduction Section of this paper.

about the effects on macroeconomic variables.[25]

The second contribution is new evidence supporting a dynamic relationship between technology news and uncertainty. I propose a nonlinear model that allows a feedback effect between the level of uncertainty and the macroeconomic and financial variables. The effects of news on consumption, GDP, investment and real personal income are amplified when the news shock hits the economy in periods of high uncertainty. The results from two counterfactuals suggest that the size of these effects depends on the initial degree of uncertainty (initial condition effect) and on how expectations about macroeconomic and financial conditions are updated (transmission effect).

The initial condition effect is in line with the idea of a 'good uncertainty' shock, that is, high uncertainty increases the likelihood of news shocks (Cascaldi-Garcia and Galvao, 2017). Periods of high uncertainty are related to a higher potential return on investment, increasing the range of growth options (Segal et al., 2015). While uncertainty reduces the utilization of production factors, it also creates an incentive to substitute less flexible for more flexible capital (Comin, 2000, Bloom, 2009, Cascaldi-Garcia and Galvao, 2017).

The transmission effect relates to how uncertainty is updated with the arrival of positive technological news (Forni et al., 2017, Berger et al., 2017). The second counterfactual shows that the positive effects of a news shock are even higher when allowing for a feedback to (and from) uncertainty. From the perspective of the news shock literature, this evidence implies that neglecting the uncertainty transmission effect leads to the conclusion that the positive effects of news shocks are weaker than they really are. From the perspective of the uncertainty literature, it raises the question of how the arrival of news, and the realization of its economic effects, influences the way economic agents update their expectations about macroeconomic and financial conditions.

[25] See Beaudry and Portier (2014) for a review of the empirical evidence of news shocks under different assumptions and identification methods.

References

Alessandri, P., and Mumtaz, H. (2014). Financial regimes and uncertainty shocks. *BCAM Working Papers*, *1404*.

Andrieu, C., Doucet, A., and Holenstein, R. (2010). Particle markov chain monte carlo methods. *Journal of the Royal Statistical Society Series* B, *72(3)*, 269–342.

Arezki, R., Ramey, V. A., and Sheng, L. (2017). News shocks in open economies: Evidence from giant oil discoveries. *The Quarterly Journal of Economics*, *132(1)*, 103–155.

Bachmann, R., Elstner, S., and Sims, E. R. (2013). Uncertainty and economic activity: Evidence from business survey data. *American Economic Journal: Macroeconomics*, *5(2)*, 217–49.

Baker, S. R., Bloom, N., and Davis, S. J. (2016). Measuring economic policy uncertainty. *NBER Working Papers, update, forthcoming: Quarterly Journal of Economics*, *21633*.

Barsky, R. B., Basu, S., and Lee, K. (2014). Whither news shocks? *NBER chapters (NBER Macroeconomics Annual 2014)*, *29*.

Barsky, R. B., and Sims, E. R. (2011). News shocks and business cycles. *Journal of Monetary Economics*, *58(3)*, 273–289.

Beaudry, P., and Portier, F. (2006). Stock prices, news, and economic fluctuations. *American Economic Review*, *96(4)*, 1293–1307.

Beaudry, P., and Portier, F. (2014). News-driven business cycles: insights and challenges. *Journal of Economic Literature*, *52(4)*, 993–1074.

Ben Zeev, N., and Khan, H. (2015). Investment-specific news shocks and U.S. business cycles. *Journal of Money, Credit and Banking*, *47(7)*, 1443–1464.

Berger, D., Dew-Becker, I., and Giglio, S. (2017). Uncertainty shocks as second-moment news shocks. *Working Paper*.

Blanchard, O. J., L'Huillier, J.-P., and Lorenzoni, G. (2013). News, noise, and fluctuations: An empirical exploration. *American Economic Review*, *103(7)*, 3045–70.

Bloom, N. (2009). The impact of uncertainty shocks. *Econometrica*, *77(3)*, 623–685.

Carriero, A., Clark, T., and Marcellino, M. (2016a). Measuring uncertainty and its impacts on the economy. *NBER-NSF Seminar on Bayesian Inference in Econometrics and Statistics*.

Carriero, A., Clark, T. E., and Marcellino, M. (2016b). Common drifting volatility in large bayesian VARs. *Journal of Business and Economic Statistics*, *34*, 375–390.

Carriero, A., Clark, T. E., and Marcellino, M. (2016c). Large vector autoregressions with stochastic volatility and flexible priors. *Federal Reserve Bank of Cleveland Working Papers*, *1617*.

Cascaldi-Garcia, D. (2017). News shocks and the slope of the term structure of interest rates: Comment. *American Economic Review*, *107(10)*, 3243–49.

Cascaldi-Garcia, D., and Galvao, A. B. (2017). News and uncertainty shocks. *WBS Working Paper*.

Christiano, L., Ilut, C. L., Motto, R., and Rostagno, M. (2010). Monetary policy and stock market booms. *Proceedings - Economic Policy Symposium - Jackson Hole, Federal Reserve Bank of Kansas City*, (pp. 85–145).

Christiano, L. J., Eichenbaum, M., and Vigfusson, R. (2003). What happens after a technology shock? *International Finance Discussion Papers - Board of Governors of the Federal Reserve System (U.S.)*, *768*.

Cogley, T., and Sargent, T. J. (2005). Drift and volatilities: Monetary policies and outcomes in the post wwii u.s. *Review of Economic Dynamics*, *8(2)*, 262–302.

Coibion, O., and Gorodnichenko, Y. (2012). What can survey forecasts tell us about information rigidities? *Journal of Political Economy*, *120(1)*, 116–159.

Comin, D. (2000). An uncertainty-driven theory of the productivity slowdown: Manufacturing. *C. V. Starr Center for Applied Economics Working Papers*, *00-16*.

Fernald, J. G. (2014). A quarterly, utilization-adjusted series on total factor productivity. *FRBSF Working Paper*, *2012-19*.

Forni, M., Gambetti, L., and Sala, L. (2014). No news in business cycles. *Economic Journal*, *124(581)*, 1168–1191.

Forni, M., Gambetti, L., and Sala, L. (2017). News, uncertainty and economic fluctuations. *CEPR Discussion Papers*, *12139*.

Francis, N., Owyang, M. T., Roush, J. E., and DiCecio, R. (2014). A flexible finite-horizon alternative to long-run restrictions with an application to technology shock. *The Review of Economics and Statistics*, *96(3)*, 638–647.

Fry, R., and Pagan, A. (2011). Sign restrictions in structural vector autoregressions: A critical review. *Journal of Economic Literature*, *49(4)*, 938–960.

Galí, J. (1999). Technology, employment, and the business cycle: Do technology shocks explain aggregate fluctuations? *American Economic Review*, *89(1)*, 249–271.

Gilchrist, S., and Zakrajšek, E. (2012). Credit spreads and business cycle fluctuations. *American Economic Review*, *102*, 1692–1720.

Görtz, C., Tsoukalas, J. D., and Zanetti, F. (2016). News shocks under financial frictions. *Working Paper*.

Jaimovich, N., and Rebelo, S. (2009). Can news about the future drive the business cycle? *American Economic Review*, *99(4)*, 1097–1118.

Jurado, K., Ludvigson, S. C., and Ng, S. (2015). Measuring uncertainty. *American Economic Review*, *105(3)*, 1177–1216.

Kim, S., Shephard, N., and Chib, S. (1998). Stochastic volatility: Likelihood inference and comparison with ARCH models. *Review of Economic Studies*, *65(3)*, 361–393.

Koop, G., Pesaran, H. M., and Potter, S. M. (1996). Impulse response analysis in non-linear multivariate models. *Journal of Econometrics*, *74(1)*, 119–147.

Kurmann, A., and Otrok, C. (2013). News shocks and the slope of the term structure of interest rates. *American Economic Review*, *103(6)*, 2612–32.

Kurmann, A., and Sims, E. (2017). Revisions in utilization-adjusted TFP and robust identification of news shocks. *NBER Working Papers*, *23142*.

Levchenko, A. A., and Pandalai-Nayar, N. (2015). TFP, news, and 'sentiments': The international transmission of business cycles. *NBER Working Papers*, *21010*.

Lindsten, F., Jordan, M. I., and Schön, T. B. (2014). Particle gibbs with ancestor sampling. *Journal of Machine Learning Research*, *15*, 2145–2184.

Ludvigson, S. C., Ma, S., and Ng, S. (2016). Uncertainty and business cycles: Exogenous impulse or endogenous response? *NBER Working Papers, update*, *21803*.

McCracken, M. W., and Ng, S. (2015). Fred-md: A monthly database for macroeconomic research. *Federal Reserve Bank of St. Louis Working Papers*, *2015-12*.

Mumtaz, H., and Theodoridis, K. (2015). Dynamic effects of monetary policy shocks on macroeconomic volatility. *Queen Mary University of London Working Papers*, *760*.

Mumtaz, H., and Zanetti, F. (2013). The impact of the volatility of monetary policy shocks. *Journal of Money, Credit and Banking*, *45(4)*, 535–558.

Ocampo, S., and Rodríguez, N. (2012). An introductory review of a structural VAR-X estimation and applications. *Revista Colombiana de Estadstica*, *35(3)*, 479–508.

Omori, Y., Chib, S., Shephard, N., and Nakajima, J. (2007). Stochastic volatility with leverage: Fast and efficient likelihood inference. *Journal of Econometrics*, *140(2)*, 425–449.

Pesaran, H. M., and Shin, Y. (1998). Generalized impulse response analysis in linear multivariate models. *Economics Letters*, *58(1)*, 17–29.

Rousseeuw, P. J., and Croux, C. (1993). Alternatives to median absolute deviation. *Journal of the American Statistical Association*, *88*, 1273–1283.

Schmitt-Grohe, S., and Uribe, M. (2012). What's news in business cycles. *Econometrica*, *80(6)*, 2733–2764.

Segal, G., Shaliastovich, I., and Yaron, A. (2015). Good and bad uncertainty: Macroeconomic and financial market implications. *Journal of Financial Economics*, *117*, 369–397.

Shen, W. (2015). News, disaster risk, and time-varying uncertainty. *Journal of Economic Dynamics and Control*, *51(C)*, 459–479.

Shin, M., and Zhong, M. (2016). A new approach to identifying the real effects of uncertainty shocks. *Finance and Economics Discussion Series, Board of Governors of the Federal Reserve System*, *2016-040*.

Uhlig, H. (2005). What are the effects of monetary policy on output? Results from an agnostic identification procedure. *Journal of Monetary Economics*, *52*, 381–419.

Vukotić, M. (2017). Sectoral effects of news shocks. *Working Paper*.

A Appendix: Triangular estimation

In this Appendix I describe the triangular estimation procedure proposed by Carriero et al. (2016c). Consider the model presented by the equation 1, but rewriting the reduced form residuals υ_t from equation 2 as

$$\begin{bmatrix} \upsilon_{1,t} \\ \upsilon_{2,t} \\ ... \\ \upsilon_{n,t} \end{bmatrix} = \begin{bmatrix} 1 & 0 & ... & 0 \\ a^*_{2,1} & 1 & ... & 0 \\ ... & ... & 1 & 0 \\ a^*_{n,1} & ... & a^*_{n,n-1} & 1 \end{bmatrix} \begin{bmatrix} \lambda^{1/2}_{1,t} & 0 & ... & 0 \\ 0 & \lambda^{1/2}_{2,t} & ... & 0 \\ ... & ... & ... & 0 \\ 0 & ... & 0 & \lambda^{1/2}_{n,t} \end{bmatrix} \begin{bmatrix} \epsilon_{1,t} \\ \epsilon_{2,t} \\ ... \\ \epsilon_{n,t} \end{bmatrix}, \tag{A.1}$$

where $a^*_{j,i}$ are the elements of the matrix $\mathbf{A}_0^{-1}$. Under this structure, it is possible to rewrite each equation of the main VAR described in 1 and variable j as

$$\begin{aligned} & y_{t,j} - (a^*_{j,1}\lambda^{1/2}_{1,t}\epsilon_{1,t} + ... + a^*_{j,j-1}\lambda^{1/2}_{j-1,t}\epsilon_{j-1,t}) \\ =& \sum_{i=1}^{n}\sum_{c=1}^{p} A^{(i)}_{j,c} y_{i,t-c} + \sum_{c=0}^{l} B_{c,j} g_{t-c} + \lambda_{j,t}\epsilon_{j,t}, \end{aligned} \tag{A.2}$$

where $A^{(i)}_{j,l}$ represents the coefficients of the matrices $\mathbf{A}_i$, and $B_{c,j}$ represents the coefficients of the matrices $\mathbf{B}_i$. The VAR can be estimated equation-by-equation following this structure by taking into account that, for equation j, the left-hand side is known *a priori*: it is the difference between $y_{t,j}$ and the residuals from the previous $(j-1)$ equations. By rescaling $y_{t,j}$ as

$$y^*_{t,j} = y_{t,j} - (a^*_{j,1}\lambda^{1/2}_{1,t}\epsilon_{1,t} + ... + a^*_{j,j-1}\lambda^{1/2}_{j-1,t}\epsilon_{j-1,t}) \tag{A.3}$$

it is possible to estimate equation A.2 as a standard generalized least squares (GLS) model.

B Appendix: Steps of the MCMC algorithm

The MCMC algorithm for this estimation follows the steps and notation proposed by Carriero et al. (2016a), which I describe here. The conditional posterior distributions for

the draws described in this Section are detailed in Appendix E.

Step 1: *Draw of the idiosyncratic volatilities.*

Rescaling υ_t as $\tilde{\upsilon}_t = \mathbf{A}_0 \upsilon_t$, combined with the linear factor model for the log-volatilities described by equation 3, it is possible to define the observation equations

$$\begin{cases} \ln(\tilde{\upsilon}_{j,t}^2 + \bar{c}) - \beta_{m,j} \ln m_t = \ln h_{j,t} + \ln \epsilon_{j,t}^2 & \text{if } j = 1, ..., n_m \\ \ln(\tilde{\upsilon}_{j,t}^2 + \bar{c}) - \beta_{f,j} \ln f_t = \ln h_{j,t} + \ln \epsilon_{j,t}^2 & \text{if } j = n_m + 1, ..., n \end{cases}, \tag{B.1}$$

where $\beta_{m,j}$ and $\beta_{f,j}$ are the loadings drawn from the previous MCMC iteration, $\bar{c}$ is a small constant in order to avoid near-zero values, and $S_{1:T}$ is the states from the 10-state mixture of normals draw from the previous iteration of the MCMC. Since $\epsilon_{j,t}$ is Gaussian with unit variance, it is possible to produce an approximate Gaussian system conditional on $S_{1:T}$.

I first produce a draw for the j states $h_{1:T}$ as

$$h_{1:T} | \Theta, S_{1:T}, m_{1:T}, f_{1:T}, \tag{B.2}$$

using the Kim et al. (1998) algorithm, where $\mathbf{\Theta}$ collects the coefficients from the matrices $\mathbf{A}_i$, $\mathbf{B}_i$, δ, $\mathbf{D}_i$, the coefficients in the conditional mean of the idiosyncratic components $\gamma = (\gamma_{j,0}, \gamma_{j,1})$, the elements of the matrix $\mathbf{A}_0$, and the elements of the volatility matrices $\mathbf{\Phi}_\upsilon$ and $\mathbf{\Phi}_u$, as in

$$\mathbf{\Theta} = (\mathbf{A}_i, \mathbf{B}_i, \delta, \mathbf{D}_i, \gamma, \mathbf{A}_0, \mathbf{\Phi}_\upsilon, \mathbf{\Phi}_u). \tag{B.3}$$

Step 2: *Draw of the factor loadings.*

Next, I produce a draw for the factor loadings $\beta_{m,j}$ and $\beta_{f,j}$, as

$$\beta_{m,j}, \beta_{f,j} | \mathbf{\Theta}, h_{1:T}, S_{1:T}, m_{1:T}, f_{1:T}. \tag{B.4}$$

The loadings can be drawn through a generalized least squares form, conditional on

the draws of $h_{1:T}$ and $S_{1:T}$, by transforming the observation equations as

$$\ln(\tilde{v}_{j,t}^2 + \bar{c}) - \ln h_{j,t} = \begin{cases} \beta_{m,j} \ln m_t + \ln \epsilon_{j,t}^2 & \text{if } j = 1, ..., n_m \\ \beta_{f,j} \ln f_t + \ln \epsilon_{j,t}^2 & \text{if } j = n_m + 1, ..., n \end{cases}. \tag{B.5}$$

Step 3: *Draw of the model coefficients and volatilities.*

The posterior coefficients and volatilities collected in $\mathbf{\Theta}$ are drawn as

$$\mathbf{\Theta} | \beta_{m,j}, \beta_{f,j}, h_{1:T}, S_{1:T}, m_{1:T}, f_{1:T}. \tag{B.6}$$

Step 4: *Draw of the macroeconomic and financial states.*

Next, the macroeconomic and financial states $m_{1:T}$ and $f_{1:T}$ are drawn as

$$m_{1:T}, f_{1:T} | \mathbf{\Theta}, \beta_{m,j}, \beta_{f,j}, h_{1:T}, S_{1:T}, \tag{B.7}$$

by employing the particle Gibbs with ancestor sampling proposed by Andrieu et al. (2010) and Lindsten et al. (2014) described in Appendix C.

Step 5: *Draw of the 10-state mixture approximation.*

Finally, I draw the 10-state mixture or normals from Omori et al. (2007) as

$$S_{1:T} | \mathbf{\Theta}, \beta_{m,j}, \beta_{f,j}, h_{1:T}, m_{1:T}, f_{1:T}. \tag{B.8}$$

C Appendix: Particle Gibbs with ancestor sampling

Consider a state space model as in

$$\ln(\tilde{v}_t^2 + \bar{c}) - \ln h_t = \ln m_t + \ln \epsilon_t^2, \quad \ln \epsilon^2 \sim \chi^2(0, s_T) \tag{C.1}$$

$$\ln m_t = D_1 \ln m_{t-1} + \delta_m \Delta y_{t-1} + u_{m,t}, \quad u_t \sim IW(0, \phi) \tag{C.2}$$

where $\ln(\tilde{v}_t^2 + \bar{c})$ is a rescaled combination of the residuals from the VAR based on the loadings β_j, $\ln h_t$ is a rescaled combination of the idiosyncratic volatilities $\ln h_{j,t}$, and $\ln \epsilon_t^2$

has a variance which is a rescaled combination of the 10-state mixture of states draw $S_{1:T}$.

Step 1: *Draw of ϕ from the IW distribution.*

Compute the error between $\ln m_t$ from the previous iteration $(i-1)$ and the predicted $\ln m_t$, as in

$$u_{m,t} = \ln m_t^{i-1} - \left(D_1 \ln m_{t-1}^{i-1} + \delta_m \Delta y_{t-1}\right). \tag{C.3}$$

Draw $\tilde{\phi}$ as following

$$\phi \sim IW\left(d_\phi \underline{\phi} + \sum_{t=1}^{T} u_{m,t}^2, d_\phi + T\right). \tag{C.4}$$

Step 2: *Compute importance weights for $t = 1$.*

Define a matrix $X_m(N,T)$, which collects the N particles. Define the first observation of the Nth particle as the first observation of m_t^{i-1}, and zero for the other particles, as in

$$X_m(N,1) = \ln m_t^{i-1}(1,1), \qquad X_m(1:(N-1),1) = 0. \tag{C.5}$$

Compute $\ln \tilde{\epsilon}_1^{2,(j)}$ for each of the $j = 1:N$ particles, as in

$$\ln \tilde{\epsilon}_1^{2,(j)} = (\ln(\tilde{v}_1^2 + \bar{c}) - \ln h_1) - X_m(j,1). \tag{C.6}$$

Compute importance weights by comparing the variance of the N particles and the $S_{1:T}$ state draw, as in

$$w(j,1) = \exp\left(-\frac{1}{2}\frac{\left(\ln \tilde{\epsilon}_1^{2,(j)}\right)^2}{S_{1:T}(1)}\right), \tag{C.7}$$

and normalizing

$$w(j,1) = \frac{w(j,1)}{\sum_{j=1}^{N} w(j,1)}. \tag{C.8}$$

Step 3: *Compute importance weights for $t = 2:T$.*

Compute N predicted m_t based on the previous particles, as in

$$\ln \tilde{m}(j,t) = \left(D_1 X_m(j,t-1) + \delta \Delta y_{t-1}\right). \tag{C.9}$$

Draw an index vector $ind(N)$ that samples the particles from $P(ind(j) = j) \propto w(1 : j, t-1)$, and ranging on the interval $[1, N]$ – these are the ancestor indexes. This index will point out which particles will be collected in the current t-step for the $N-1$ first particles. Store the particles as in

$$X_n(j,t) = \ln \tilde{m}(ind(j),t) + \tilde{\phi}^{1/2} * randn(1,1), \tag{C.10}$$

and set the Nth particle as the previous iteration $(i-1)$ value for m_t

$$X_m(N,t) = \ln m_t^{i-1}(1,t). \tag{C.11}$$

Compute $\ln \tilde{\epsilon}_1^{2,(j)}$ for each of the $j = 1 : N$ particles as before, following

$$\ln \tilde{\epsilon}_t^{2,(j)} = (\ln(\tilde{v}_t^2 + \bar{c}) - \ln h_t) - X_m(j,t), \tag{C.12}$$

the importance weights as

$$w(j,t) = \exp\left(-\frac{1}{2}\frac{\left(\ln \tilde{\epsilon}_t^{2,(j)}\right)^2}{S_{1:T}(t)}\right), \tag{C.13}$$

and normalizing

$$w(j,t) = \frac{w(j,t)}{\sum_{j=1}^{N} w(j,t)}. \tag{C.14}$$

The last part of this step is defining the Nth ancestor index. In a conventional Particle Gibbs, this is done by simply assigning $ind(N) = N$, ensuring that $m_t^{i-1}(1,t)$ from the previous iteration is one of the particles. With the ancestor sampling, a new value for $ind(N)$ is sampled to artificially assign a history to this partial path, by connecting $m_t^{i-1}(1,t)$ to one of the particles. Formally, this sample is done by computing

$$w_{ind}(j,t) = w(j,t-1) * \exp\left(-\frac{1}{2}\frac{\left(m_t^{i-1}(1,t) - \tilde{m}(j,t)\right)^2}{\tilde{\phi}}\right), \tag{C.15}$$

normalizing

$$w_{ind}(j,t) = \frac{w_{ind}(j,t)}{\sum_{j=1}^{N} w_{ind}(j,t)}, \tag{C.16}$$

and drawing $ind(N)$ from $P(ind(N) = j) \propto w_{ind}(j,t)$. Finally, store the ancestor indexes in a matrix $a(N,T)$ as $a(1:N,t) = ind(1:N)$.

Step 4: *Compute the final filtered* m_t^i.

Rearrange $X_m(j,t)$ in order to generate the trajectories of the N particles based on the ancestor indexes stored in $a(N,T)$ following the last ordering $a(j,T)$. Draw an indicator J from $P(J = j) \propto w(j,1:T)$, and set $\ln m_t^i = X_m(J,1:T)$.

D Appendix: State-space representation

The model described by equations 1 and 5 can be combined and rewritten in a state-space representation. This transformation makes it easier to check the stationarity of the system and to compute impulse responses.

Consider a model in which the macroeconomic and financial factors only depend on their previous values ($\mathbf{D}_i$ lag order is $k = 1$) and on Δy_{t-1}. Equation 5 becomes

$$g_t = \mathbf{D}_1 g_{t-1} + \delta \Delta y_{t-1} + u_t, \tag{D.1}$$

or simply

$$g_t = \mathbf{D}_1 g_{t-1} + \delta y_{t-1} - \delta y_{t-2} + u_t. \tag{D.2}$$

Consider now that the main VAR (equation 1) has lag order of y_t of p, $l = 1$ lag of the macro and financial factors g_t, and $v_t = \mathbf{A}_0^{-1} \mathbf{\Lambda}_t^{1/2} \epsilon_t$. Rewrite equation 1 as

$$y_t = \mathbf{A}_1 y_{t-1} + ... + \mathbf{A}_p y_{t-p} + \mathbf{B}_0 g_t + \mathbf{B}_1 g_{t-1} + \mathbf{A}_0^{-1} \mathbf{\Lambda}_t^{1/2} \epsilon_t, \tag{D.3}$$

substituting g_t from equation D.2 in equation D.3, results in

$$\begin{aligned} y_t &= \mathbf{A}_1 y_{t-1} + ... + \mathbf{A}_p y_{t-p} + \mathbf{B}_0(\mathbf{D}_1 g_{t-1} + \delta y_{t-1} - \delta y_{t-2} + u_t) + ... \\ &... + \mathbf{B}_1 g_{t-1} + \mathbf{A}_0^{-1} \mathbf{\Lambda}_t^{1/2} \epsilon_t, \end{aligned} \tag{D.4}$$

which can be rearranged as

$$\begin{aligned} y_t &= (\mathbf{A}_1 + \mathbf{B}_0\delta) y_{t-1} + (\mathbf{A}_2 - \mathbf{B}_0\delta) y_{t-2} + ... + \mathbf{A}_p y_{t-p} + ... \\ &... + (\mathbf{B}_1 + \mathbf{B}_0\mathbf{D}_1) g_{t-1} + \mathbf{B}_0 u_t + \mathbf{A}_0^{-1} \mathbf{\Lambda}_t^{1/2} \epsilon_t. \end{aligned} \tag{D.5}$$

Now, this equation can be conveniently written in a state-space form as in

$$\begin{bmatrix} y_t \\ y_{t-1} \\ ... \\ y_{t-p} \\ g_t \end{bmatrix} = \underbrace{\begin{bmatrix} \mathbf{F}_1 & \mathbf{F}_2 & ... & \mathbf{F}_3 & \mathbf{F}_4 \\ \mathbf{I}_n & 0 & ... & 0 & 0 \\ ... & ... & ... & ... & ... \\ 0 & 0 & ... & \mathbf{I}_n & 0 \\ \delta & -\delta & ... & 0 & \mathbf{D}_1 \end{bmatrix}}_{\mathbf{F}} \begin{bmatrix} y_{t-1} \\ y_{t-2} \\ ... \\ y_{t-p-1} \\ g_{t-1} \end{bmatrix} + \begin{bmatrix} \mathbf{A}_0^{-1}\mathbf{\Lambda}_t^{1/2} & 0 & ... & 0 & \mathbf{B}_0 \\ 0 & 0 & 0 & 0 & 0 \\ ... & ... & ... & ... & ... \\ 0 & 0 & 0 & 0 & 0 \\ 0 & 0 & 0 & 0 & \mathbf{I}_2 \end{bmatrix} \begin{bmatrix} \epsilon_t \\ 0 \\ ... \\ 0 \\ u_t \end{bmatrix}, \tag{D.6}$$

where

$$\begin{aligned} \mathbf{F}_1 &= (\mathbf{A}_1 + \mathbf{B}_0\delta), \\ \mathbf{F}_2 &= (\mathbf{A}_2 - \mathbf{B}_0\delta), \\ \mathbf{F}_3 &= \mathbf{A}_p, \\ \mathbf{F}_4 &= (\mathbf{B}_1 + \mathbf{B}_0\mathbf{D}_1). \end{aligned} \tag{D.7}$$

The matrix $\mathbf{\Lambda}_t$ takes the form

$$\mathbf{\Lambda}_t = \begin{bmatrix} \lambda_{1,t} & 0 & ... & 0 \\ 0 & \lambda_{2,t} & ... & 0 \\ 0 & 0 & ... & \lambda_{n,t} \end{bmatrix}, \tag{D.8}$$

where each of its coefficients are a combination of an idiosyncratic shock $h_{j,t}$ and either a macroeconomic factor m_t or a financial factor f_t, as in

$$\lambda_{j,t} = \begin{cases} m_t^{\beta_{m,j}} h_{j,t} & \text{if } j = 1, ..., n_m \\ f_t^{\beta_{f,j}} h_{j,t} & \text{if } j = n_m + 1, ..., n \end{cases}, \tag{D.9}$$

where the log of the idiosyncratic shocks $\ln h_{j,t}$ follow an $AR(1)$ process as in

$$\ln h_{j,t} = \gamma_{j,0} + \gamma_{j,1} \ln h_{j,t-1} + e_{j,t}, \quad j = 1, ..., n. \tag{D.10}$$

E Appendix: Priors and conditional posteriors

Here I present the prior and conditional posterior distributions for the parameters and coefficients for the MCMC steps explained in Appendix B. I follow the proposed priors and notation from Carriero et al. (2016a), with priors defined as

$$vec(\mathbf{A}_i; \mathbf{B}_i) \sim N(vec(\underline{\mu}_A), \underline{\mathbf{\Omega}}_A), \quad i = 1, ..., p, \tag{E.1}$$

$$a_j \sim N(\underline{\mu}_{a,j}, \underline{\mathbf{\Omega}}_{a,j}), \quad j = 2, ..., n, \tag{E.2}$$

$$\beta_j \sim N(\underline{\mu}_\beta, \underline{\mathbf{\Omega}}_\beta), \quad j = 2, ..., n_m, n_{m+2}, ..., n, \tag{E.3}$$

$$\gamma_j \sim N(\underline{\mu}_\gamma, \underline{\mathbf{\Omega}}_\gamma), \quad j = 1, ..., n, \tag{E.4}$$

$$\delta \sim N(\underline{\mu}_\delta, \underline{\mathbf{\Omega}}_\delta), \tag{E.5}$$

$$\phi_j \sim IG(d_\phi \underline{\phi}, d_\phi), \quad j = 1, ..., n, \tag{E.6}$$

$$\mathbf{\Phi}_u \sim IW(d_{\Phi_u} \underline{\mathbf{\Phi}}_u, d_{\Phi_u}). \tag{E.7}$$

Under these priors, the posterior conditional distributions follow

$$vec(\mathbf{A}_i; \mathbf{B}_i) | \mathbf{A}_0, \beta, m_{1:T}, f_{1:T}, h_{1:T}, y_{1:T} \sim N(vec(\bar{\mu}_A), \bar{\mathbf{\Omega}}_A), \quad i = 1, ..., p, \tag{E.8}$$

$$a_j|\mathbf{A}_i, \mathbf{B}_i, \beta, m_{1:T}, f_{1:T}, h_{1:T}, y_{1:T} \sim N(\bar{\mu}_{a,j}, \bar{\mathbf{\Omega}}_{a,j}), \quad j = 2, ..., n, \tag{E.9}$$

$$1\beta_j|\mathbf{A}_i, \mathbf{A}_0, \mathbf{B}_i, \gamma, \mathbf{\Phi}, \beta, m_{1:T}, f_{1:T}, S_{1:T}, y_{1:T} \sim N(\underline{\mu}_\beta, \underline{\mathbf{\Omega}}_\beta), \quad j = 2, ..., n_m, n_{m+2}, ..., n, \tag{E.10}$$

$$\gamma_j|\mathbf{A}_i, \mathbf{A}_0, \mathbf{B}_i, \mathbf{\Phi}, \beta, m_{1:T}, f_{1:T}, h_{1:T}, y_{1:T} \sim N(\underline{\mu}_\gamma, \underline{\mathbf{\Omega}}_\gamma), \quad j = 1, ..., n, \tag{E.11}$$

$$\delta|\mathbf{A}_i, \mathbf{A}_0, \mathbf{B}_i, \mathbf{\Phi}, \gamma, \beta, m_{1:T}, f_{1:T}, h_{1:T}, y_{1:T} \sim N(\underline{\mu}_\delta, \underline{\mathbf{\Omega}}_\delta), \tag{E.12}$$

$$\phi_j|\mathbf{A}_i, \mathbf{A}_0, \mathbf{B}_i, \gamma, \beta, m_{1:T}, f_{1:T}, h_{1:T}, y_{1:T} \sim IG(d_\phi \underline{\phi}, d_\phi), \quad j = 1, ..., n, \tag{E.13}$$

$$\Phi_u|\mathbf{A}_i, \mathbf{A}_0, \mathbf{B}_i, \gamma, \beta, \delta, m_{1:T}, f_{1:T}, h_{1:T}, y_{1:T} \sim IW(d_{\Phi_u} \underline{\mathbf{\Phi}}_u, d_{\Phi_u}). \tag{E.14}$$

The posterior $\bar{\mu}_A$ is drawn equation-by-equation through the triangularization method described in Section A. The posteriors $\bar{\mu}_{a,j}$, $\bar{\mu}_\delta$ and $\bar{\mu}_\gamma$ follow the results from the standard linear regression model. The factor loadings β are drawn following a GLS-based form depending on the mixture states drawn for the volatilities, as in Carriero et al. (2016a).

With regard to the priors, I adopt a Minnesota-type structure for the VAR coefficients in $\mathbf{A}_i$. This model contains stationary and non-stationary variables, so the prior coefficients of the stationary variables are set to 0, while the prior coefficients of the non-stationary variables are set to 1. The variance-covariance matrix $\underline{\mathbf{\Omega}}_A$ is diagonal, with standard Minnesota shrinkage form, as in

$$\underline{\mathbf{\Omega}}_A = var[\underline{A}_k^{ij}] = \begin{cases} \left(\frac{\theta_1^2}{l^2}\right) & \text{if } i = j, \\ \left(\frac{\theta_1 \theta_2}{l} \frac{\sigma_i}{\sigma_j}\right)^2, & \text{if } i = j, \\ (\theta_0 \sigma_i)^2, & \text{if intercept or } g_t. \end{cases} \tag{E.15}$$

where l is the lag. The overall prior tightness θ_1 is set here as 0.05, the cross-shrinkage parameter θ_2 is set to 0.5 and the intercept shrinkage parameter θ_0 is set to 1,000. I follow Carriero et al. (2016a) by also setting a prior variance for the uncertainty factors $\ln m_t$ and $\ln f_t$ equal to the intercept. The variance parameters σ_i come from the residual variances of an $AR(p)$ process for each variable.

The prior means and variances for the remainder of the coefficients are presented in

Table E.1.

Table E.1 Mean and variance priors

	Mean	**Variance**	**Degree of freedom**
a_j	0	10	-
$(\gamma_{i,0}, \gamma_{i,1})$	$(\ln \sigma_i^2, 0)$	$(2, 0.4^2)$	-
β_j, for $j = 2, ..., n_m$, and $j = n_{m+2}, ...n$	1	0.4^2	-
$\mathbf{D}_i$	0.8, for first own lag, 0 otherwise	0.2^2	-
δ	0	0.1^2	-
ϕ_j	0.03	-	10
$\mathbf{\Phi}_u$	$0.01 I_n$		10
$\ln m_0$ and $\ln f_0$	0	-	-
$\ln h_{i,0}$	$\ln \sigma_i^2$	2	-

There is discussion in the literature on the impact of the prior on the components a_j of matrix $\mathbf{A}_0$. The model may be dependent on the ordering of the variables, along with the priors imposed on a_j. This is an issue primarily in using this model for forecasting purposes. I address these questions by following Carriero et al. (2016a) and Cogley and Sargent (2005) and imposing a prior fairly uninformative for a_j, with mean of 0 and variances of 10. In addition, the identification procedure of maximizing the variance decomposition over a predefined forecast period is order-invariant, avoiding the problem of choosing the wrong order of variables.

Finally, the dependence of the uncertainty factors on lagged values of y_t creates an (indirect) extra dependency of current values of y_t to lagged values not captured by the main VAR. This dependency is clearly noticed when the main VAR is rewritten in a state-space model, as in equation D.6, where the coefficients δ are also part of $\mathbf{F}_1$ and $\mathbf{F}_2$. I follow strategy similar to Mumtaz and Theodoridis (2015) by imposing additional shrinkage to the variance of δ, which I set to $\left(\frac{\theta_1^2}{l^2}\right)$.

F Appendix: Generalized impulse responses procedure

In this Appendix I present the procedure of estimating the generalized impulse responses for the news shock and the uncertainty shocks.

Due to the non-linearity that the time-varying volatilities bring to the model, the feedback effect that the variables cause to the volatility through the uncertainty factors, and the feedback of the uncertainty factors on the mean of the variables, it is not possible to employ a conventional impulse response setting in this case. The strategy here is to use an adaptation of the procedure proposed by Koop et al. (1996) and Pesaran and Shin (1998), taking into account that the shocks $v_t = \mathbf{A}_0^{-1}\mathbf{\Lambda}_t^{1/2}\epsilon_t$ are orthogonal by construction.

The idea is to create two distinct forecast paths for the variables y_t, a baseline and a shocked containing the shock of interest (namely, τ_j). The generalized impulse responses are the difference between these two paths. To accomplish this, it is necessary to construct a set of random shocks $\omega_{j,t}$ over the forecast period that mimic the behavior of ϵ_t. The generalized impulse response (GI) of a r set of randomly drawn $\omega_{j,t}^r$ is given by

$$GI^r(k, \tau_j, \omega_{j,t}^r, \mathbf{Z}_t, \mathbf{\Pi}) = \mathbb{E}[y_{t+k}^r|\tau_j, \omega_{j,t}^r, \mathbf{Z}_t, \mathbf{\Pi}] - \mathbb{E}[y_{t+k}^r|\omega_{j,t}, \mathbf{Z}_t, \mathbf{\Pi}], \tag{F.1}$$

where k is the forecast point in time, $\mathbf{Z}_t$ is the information set containing all the known history up to time t defined as $\mathbf{Z}_t = (y_{t-p}, ..., y_t; g_{t-p}, .., g_t)$,[26] $\mathbf{\Pi}$ collects the coefficient matrices as $\mathbf{\Pi} = [\mathbf{A}_i, \mathbf{B}_i, \mathbf{D}_i, \beta_j, \gamma_j, \delta]$, $\mathbb{E}[y_{t+k}^r|\tau_j, \omega_{j,t}^r, \mathbf{Z}_t]$ is the shocked path of y_t and $\mathbb{E}[y_{t+k}^r|\omega_{j,t}^r, \mathbf{Z}_t]$ is the baseline path of the baseline path of y_t.

Repeat the procedure of equation F.1 R times, and take the averages over R of these paths. Koop et al. (1996) show that as $R \to \infty$, by the Law of Large Numbers these averages will converge the conditional expectations $\mathbb{E}[y_{t+k}|\tau_j, \mathbf{Z}_t, \mathbf{\Pi}]$ and $\mathbb{E}[y_{t+k}|\mathbf{Z}_t, \mathbf{\Pi}]$,

[26] Where $g_t = (\ln m_t; \ln f_t)$.

and the generalized impulse response can be constructed as

$$GI(k, \tau_j, \mathbf{Z}_t, \mathbf{\Pi}) = \mathbb{E}[y_{t+k}|\tau_j, \mathbf{Z}_t, \mathbf{\Pi}] - \mathbb{E}[y_{t+k}|\mathbf{Z}_t, \mathbf{\Pi}]. \tag{F.2}$$

F.1 Generalized impulse responses for a news shock

For the news shock case, I start with the state-space procedure presented in equations D.6 and D.9 (Appendix D). The news shock is identified as the orthogonalization of the shocks on the mean of the variables that maximize the variance decomposition of one objective variable over a predefined forecast period. It follows that the identification relies on an orthogonalization of the innovations ϵ_t. By construction, ϵ_t is independent from the idiosyncratic innovations $e_{j,t}$ and the uncertainty innovations $u_{m,t}$ and $u_{f,t}$. Since I am only interested in ϵ_t for the news shock identification, I set $e_{j,t} = 0$, $u_{m,t} = 0$ and $u_{f,t} = 0$ in this procedure.

With this simplification, it is possible to rewrite equations D.6 and D.9, respectively, as

$$\begin{bmatrix} y_t \\ y_{t-1} \\ ... \\ y_{t-p} \\ g_t \end{bmatrix} = \underbrace{\begin{bmatrix} \mathbf{F}_1 & \mathbf{F}_2 & ... & \mathbf{F}_3 & \mathbf{F}_4 \\ \mathbf{I}_n & 0 & ... & 0 & 0 \\ ... & ... & ... & ... & ... \\ 0 & 0 & ... & \mathbf{I}_n & 0 \\ \delta & -\delta & ... & 0 & \mathbf{D}_1 \end{bmatrix}}_{\mathbf{F}} \begin{bmatrix} y_{t-1} \\ y_{t-2} \\ ... \\ y_{t-p-1} \\ g_{t-1} \end{bmatrix} + \begin{bmatrix} \mathbf{A}_0^{-1}\mathbf{\Lambda}_t^{1/2} & 0 & ... & 0 & \mathbf{B}_0 \\ 0 & 0 & 0 & 0 & 0 \\ ... & ... & ... & ... & ... \\ 0 & 0 & 0 & 0 & 0 \\ 0 & 0 & 0 & 0 & \mathbf{I}_2 \end{bmatrix} \begin{bmatrix} \epsilon_t \\ 0 \\ ... \\ 0 \\ 0 \end{bmatrix}, \tag{F.3}$$

and

$$\ln h_{j,t} = \gamma_{j,0} + \gamma_{j,1} \ln h_{j,t-1}, \quad j = 1, ..., n. \tag{F.4}$$

Now that the model has only a single set of innovations ϵ_t, the generalized impulse responses for the news shock can be constructed with the following steps. The identification of the news shock is dependent on the total variance, and the variance changes over time, so the following procedure is executed at each point in time. This allows the

construction of a time-varying identification, with different impulse responses at every point in the time span considered.

Step 1: *Construct a baseline path.*

Considering one draw r of the random innovations $\omega_{j,t}^r$ and K being the forecast period, construct by simulation a baseline path from $t+1$ to $t+K$ for the idiosyncratic innovations $\ln h_{j,t}^r$ using equation F.4, and for $y_{t,base}^r$, $g_{t,base}^r$[27] and $\mathbf{\Lambda}_{t,base}^r$ using equation F.3.

Step 2: *Construct a shocked path for a utilization-adjusted TFP shock.*

Take the same draw r from Step 1, and the idiosyncratic innovations $\ln h_{j,t}^r$. For $t+1$, construct a one standard deviation shock on utilization-adjusted TFP by adding to $\omega_{j,t+1}^r$ the shock τ_{TFP}^r, which is a vector with 1 in the first position (where utilization-adjusted TFP ordered first in the VAR) and zeros elsewhere. Construct by simulation a TFP shocked path from $t+1$ to $t+K$ for $y_{TFP,t}^r$, $g_{TFP,t}^r$[28] and $\mathbf{\Lambda}_{TFP,t}^r$ using equation F.3.

Step 3: *Construct the impulse responses for a TFP shock.*

Following equation F.1, construct the impulse responses for a utilization-adjusted TFP shock as the differences between the shocked and the baseline paths for the draw r as

$$\begin{aligned} GI_{TFP,t}^r(k, \tau_{TFP}^r, \omega_{j,t}^r, \mathbf{Z}_t, \mathbf{\Pi}) = \mathbb{E}[y_{t+k,TFP}^r, g_{t+k,TFP}^r | \tau_{TFP}^r, \mathbf{\Lambda}_{t+k,TFP}^r, \omega_{j,t}^r, \mathbf{Z}_t, \mathbf{\Pi}] \\ - \mathbb{E}[y_{t+k,base}^r, g_{t+k,base}^r | \mathbf{\Lambda}_{t+k,base}^r, \omega_{j,t}^r, \mathbf{Z}_t, \mathbf{\Pi}]. \end{aligned} \tag{F.5}$$

Step 4: *Identify the news shock.*

Identify the news shock for the draw r as the orthogonalization on ϵ_t that maximizes the variance decomposition of utilization-adjusted TFP over a predefined K forecast period.[29] The idea of identifying the news shock for every r draw is in line with the discussion about the difference between structural and model identification from Fry and Pagan (2011). Every r draw is a realization of a different model among infinite alternative models, leading to unique identification of the news shock. The best approximation of

[27] Where $g_{t,base} = (\ln m_{t,base}; \ln f_{t,base})$.
[28] Where $g_{t,TFP} = (\ln m_{t,TFP}; \ln f_{t,TFP})$.
[29] For this paper, I follow Barsky and Sims (2011) and set $K = 40$ quarters ahead.

the structural identification will be the average across all r impulse responses after the news shock is properly identified for each different model.

Following the identification procedure proposed in Section 3.1, the news shock $\tau^r_{t,news}$ can be identified as

$$\tau^r_{t,news} = \arg\max \frac{\sum_{k=0}^{K} GI^r_{TFP,t}(k, \tau^r_{TFP}, \omega^r_{j,t}, \mathbf{Z}_t, , \mathbf{\Pi}, \tau) GI^r_{TFP,t}(k, \tau^r_{TFP}, \omega^r_{j,t}, \mathbf{Z}_t, , \mathbf{\Pi}, \tau)'}{\sum_{k=0}^{K} \mathbf{B}_1 A^{-1} \Lambda^{1/2}_{t+k,TFP} (A^{-1} \Lambda^{1/2}_{t+k,TFP})' \mathbf{B}_1'}, \tag{F.6}$$

subject to

$$\begin{aligned} & A^{-1}(1,j) = 0, \quad \forall j > 1, \\ & \tau(1,1) = 0, \\ & \tau'\tau = 1, \end{aligned} \tag{F.7}$$

where $\mathbf{B}_1$ is the line correspondent to the utilization-adjusted TFP coefficients in the state-space representation described in equation D.6 (Appendix D).

Step 5: *Construct a shocked path for the news shock.*

Take the same draw r from Step 1, and the idiosyncratic innovations $\ln h^r_{j,t}$. For $t+1$, construct a TFP news shock by adding the shock $\tau^r_{t,news}$ to $\omega^r_{j,t+1}$. Construct by simulation a news shocked path from $t+1$ to $t+K$ for $y^r_{t,news}$, $g^r_{t,news}$[30] and $\mathbf{\Lambda}^r_{t,news}$ using equation F.3.

Step 6: *Construct the impulse responses for the news shock.*

Following equation F.1, construct the impulse responses for the news shock as the differences between the shocked news path and the baseline path from Step 1 for the draw r as

$$\begin{aligned} GI^r_{t,news}(k, \tau^r_{t,news}, \omega^r_{j,t}, \mathbf{Z}_t, \mathbf{\Pi}) = & \mathbb{E}[y^r_{t+k,news}, g^r_{t+k,news} | \tau^r_{t,news}, \mathbf{\Lambda}^r_{t+k,news}, \omega^r_{j,t}, \mathbf{Z}_t, \mathbf{\Pi}] \\ & - \mathbb{E}[y^r_{t+k,base}, g^r_{t+k,base} | \mathbf{\Lambda}^r_{t+k,base}, \omega_{j,t}, \mathbf{Z}_t, \mathbf{\Pi}]. \end{aligned} \tag{F.8}$$

Step 7: *Construct the average impulse responses for the news shock.*

Repeat Steps 1 to 6 for R number of times and form the averages of the shocked news

[30] Where $g_{t,news} = (\ln m_{t,news}; \ln f_{t,news})$.

and baseline paths across all R draws of ω_{j,t^r} as

$$\begin{aligned}
\bar{y}_{t+k,news}(k, \tau_{t,news}, \mathbf{Z}_t, \mathbf{\Pi}) &= \frac{1}{R}\sum_{r=1}^{R} y^r_{t+k,news}(\tau^r_{t,news}, \mathbf{\Lambda}^r_{t+k,news}, \omega^r_{j,t}, \mathbf{Z}_t, \mathbf{\Pi}), \\
\bar{g}_{t+k,news}(k, \tau_{t,news}, \mathbf{Z}_t, \mathbf{\Pi}) &= \frac{1}{R}\sum_{r=1}^{R} g^r_{t+k,news}(\tau^r_{t,news}, \mathbf{\Lambda}^r_{t+k,news}, \omega^r_{j,t}, \mathbf{Z}_t, \mathbf{\Pi}), \\
\bar{y}_{t+k,base}(k, \mathbf{Z}_t, \mathbf{\Pi}) &= \frac{1}{R}\sum_{r=1}^{R} y^r_{t+k,base}(\mathbf{\Lambda}^r_{t+k,base}, \omega^r_{j,t}, \mathbf{Z}_t, \mathbf{\Pi}), \\
\bar{g}_{t+k,base}(k, \mathbf{Z}_t, \mathbf{\Pi}) &= \frac{1}{R}\sum_{r=1}^{R} g^r_{t+k,base}(\mathbf{\Lambda}^r_{t+k,base}, \omega^r_{j,t}, \mathbf{Z}_t, \mathbf{\Pi}).
\end{aligned} \tag{F.9}$$

Lastly, construct the final generalized impulse responses for the news shock as the differences between these averages, as in

$$\begin{aligned}
GI_{t,news}(k, \tau_{t,news}, \mathbf{Z}_t, \mathbf{\Pi}) = &[\bar{y}_{t+k,news}(k, \tau_{t,news}, \mathbf{Z}_t, \mathbf{\Pi}), \bar{g}_{t+k,news}(k, \tau_{t,news}, \mathbf{Z}_t, \mathbf{\Pi})] \\
&- [\bar{y}_{t+k,base}(k, \mathbf{Z}_t, \mathbf{\Pi}), \bar{g}_{t+k,base}(k, \mathbf{Z}_t, \mathbf{\Pi})].
\end{aligned} \tag{F.10}$$

After testing different R sizes, I set $R = 1,000$ for this paper. Since changing from $R = 1,000$ to $R = 5,000$ did not present any noticeable difference, $R = 1,000$ is sufficiently large to achieve the difference between conditional expectations expressed in equation F.2.

F.2 Generalized impulse responses for uncertainty shocks

Here I describe the procedure for constructing the generalized impulse responses to macro and financial uncertainty shocks.

Step 1: *Construct a baseline path.*

Considering one draw r of the random innovations $\omega^r_{j,t}$ and K being the forecast period, construct by simulation a baseline path from $T+1$ to $T+K$ for the idiosyncratic innovations $\ln h^r_{j,t}$ using equation F.4, and for $y^r_{t,base}$, $g^r_{t,base}$ and $\mathbf{\Lambda}^r_{t,base}$ using equation F.3.

Step 2: *Construct a shocked path for each of the uncertainty shocks.*

Take the same draw r from Step 1, and the idiosyncratic innovations $\ln h^r_{j,t}$. Construct

the macro and financial shocks through a lower triangular Cholesky decomposition as

$$\begin{aligned}\tau^r_{macro} &= chol(\mathbf{\Phi}_u, \text{'lower'}) * q_i^{macro},\\ \tau^r_{fin} &= chol(\mathbf{\Phi}_u, \text{'lower'}) * q_i^{fin},\end{aligned} \tag{F.11}$$

where q_i^{macro} is a 2×1 vector with 1 in the first position and zero in the second, and q_i^{fin} is a 2×1 vector with zero in the first position and 1 in the second. For $T+1$, construct a one standard deviation shock on macro uncertainty by substituting $(u_{m,t}, u_{f,t})'$ in equation D.6 for τ^r_{macro}. Construct by simulation a macro shocked path from $T+1$ to $T+K$ for $y^r_{t,macro}$, $g^r_{t,macro}$ and $\mathbf{\Lambda}^r_{t,macro}$ using equation D.6. Repeat the process for the financial uncertainty by using τ^r_{fin} to construct paths for $y^r_{t,fin}$, $g^r_{t,fin}$ and $\mathbf{\Lambda}^r_{t,fin}$.

Step 3: *Construct the impulse responses for the uncertainty shocks.*

Following equation F.1, construct the impulse responses for the macro and financial shocks as the differences between the shocked and the baseline paths for the draw r as

$$\begin{aligned}GI^r_{macro}(k, \tau^r_{macro}, \omega^r_{j,t}, \mathbf{Z}_T, \mathbf{\Pi}) &= \mathbb{E}[y^r_{T+k,macro}, g^r_{T+k,macro} | \tau^r_{macro}, \mathbf{\Lambda}^r_{T+k,macro}, \omega^r_{j,t}, \mathbf{Z}_T, \mathbf{\Pi}]\\ &\quad - \mathbb{E}[y^r_{T+k,base}, g^r_{T+k,base} | \mathbf{\Lambda}^r_{T+k,base}, \omega^r_{j,t}, \mathbf{Z}_T, \mathbf{\Pi}],\\ GI^r_{fin}(k, \tau^r_{fin}, \omega^r_{j,t}, \mathbf{Z}_T, \mathbf{\Pi}) &= \mathbb{E}[y^r_{T+k,fin}, g^r_{T+k,fin} | \tau^r_{fin}, \mathbf{\Lambda}^r_{T+k,fin}, \omega^r_{j,t}, \mathbf{Z}_T, \mathbf{\Pi}]\\ &\quad - \mathbb{E}[y^r_{T+k,base}, g^r_{T+k,base} | \mathbf{\Lambda}^r_{T+k,base}, \omega^r_{j,t}, \mathbf{Z}_T, \mathbf{\Pi}].\end{aligned} \tag{F.12}$$

Step 4: *Construct the average impulse responses for the uncertainty shocks.*

Repeat Steps 1 to 3 for R number of times and form the averages of the shocked and

baseline paths across all R draws of ω_{j,t^r} as

$$\begin{aligned}
\bar{y}_{t+k,macro}(k,\tau_{t,macro},\mathbf{Z}_t,\mathbf{\Pi}) &= \frac{1}{R}\sum_{r=1}^{R} y^r_{t+k,macro}(\tau^r_{t,macro},\mathbf{\Lambda}^r_{t+k,macro},\omega^r_{j,t},\mathbf{Z}_t,\mathbf{\Pi}),\\
\bar{y}_{t+k,fin}(k,\tau_{t,fin},\mathbf{Z}_t,\mathbf{\Pi}) &= \frac{1}{R}\sum_{r=1}^{R} y^r_{t+k,fin}(\tau^r_{t,fin},\mathbf{\Lambda}^r_{t+k,fin},\omega^r_{j,t},\mathbf{Z}_t,\mathbf{\Pi}),\\
\bar{g}_{t+k,macro}(k,\tau_{t,macro},\mathbf{Z}_t,\mathbf{\Pi}) &= \frac{1}{R}\sum_{r=1}^{R} g^r_{t+k,macro}(\tau^r_{t,macro},\mathbf{\Lambda}^r_{t+k,macro},\omega^r_{j,t},\mathbf{Z}_t,\mathbf{\Pi}),\\
\bar{g}_{t+k,fin}(k,\tau_{t,fin},\mathbf{Z}_t,\mathbf{\Pi}) &= \frac{1}{R}\sum_{r=1}^{R} g^r_{t+k,fin}(\tau^r_{t,fin},\mathbf{\Lambda}^r_{t+k,fin},\omega^r_{j,t},\mathbf{Z}_t,\mathbf{\Pi}),\\
\bar{y}_{t+k,base}(k,\mathbf{Z}_t,\mathbf{\Pi}) &= \frac{1}{R}\sum_{r=1}^{R} y^r_{t+k,base}(\mathbf{\Lambda}^r_{t+k,base},\omega^r_{j,t},\mathbf{Z}_t,\mathbf{\Pi}),\\
\bar{g}_{t+k,base}(k,\mathbf{Z}_t,\mathbf{\Pi}) &= \frac{1}{R}\sum_{r=1}^{R} g^r_{t+k,base}(\mathbf{\Lambda}^r_{t+k,base},\omega^r_{j,t},\mathbf{Z}_t,\mathbf{\Pi}).
\end{aligned} \tag{F.13}$$

Lastly, construct the final generalized impulse responses for the macro and financial shocks as the differences between these averages, as in

$$\begin{aligned}
GI_{t,macro}(k,\tau_{t,macro},\mathbf{Z}_t,\mathbf{\Pi}) &= [\bar{y}_{t+k,macro}(k,\tau_{t,macro},\mathbf{Z}_t,\mathbf{\Pi}),\bar{g}_{t+k,macro}(k,\tau_{t,macro},\mathbf{Z}_t,\mathbf{\Pi})]\\
&\quad - [\bar{y}_{t+k,base}(k,\mathbf{Z}_t,\mathbf{\Pi}),\bar{g}_{t+k,base}(k,\mathbf{Z}_t,\mathbf{\Pi})],\\
GI_{t,fin}(k,\tau_{t,fin},\mathbf{Z}_t,\mathbf{\Pi}) &= [\bar{y}_{t+k,fin}(k,\tau_{t,fin},\mathbf{Z}_t,\mathbf{\Pi}),\bar{g}_{t+k,fin}(k,\tau_{t,fin},\mathbf{Z}_t,\mathbf{\Pi})]\\
&\quad - [\bar{y}_{t+k,base}(k,\mathbf{Z}_t,\mathbf{\Pi}),\bar{g}_{t+k,base}(k,\mathbf{Z}_t,\mathbf{\Pi})].
\end{aligned} \tag{F.14}$$

As it is the case for the news shock, I set $R = 1,000$ for the uncertainty shocks, which is enough to achieve the difference between conditional expectations expressed in equation F.2.

G Appendix: Data description

Table G.1 Description of macroeconomic variables

	Name	Description	Source
1	Utilization-adjusted TFP	Utilization-adjusted TFP in log levels. Computed by Fernald (2014).	Fernald's website (Nov/2015)
2	Consumption	Real per capita consumption in log levels. Computed using PCE (nondurable goods + services), price deflator and population.	Fred
3	Output	Real per capita GDP in log levels. Computed using the real GDP (business, nonfarm) and population.	Fred
4	Investment	Real per capita investment in log levels. Computed using PCE durable goods + gross private domestic investment, price deflator and population.	Fred
5	Hours	Per capita hours in log levels. Computed with Total hours in nonfarm business sector and population values.	Fred
6	Prices	Price deflator, computed with the implicit price deflator for nonfarm business sector.	Fred
7	FFR	Fed funds rate.	Fred
8	Payroll	Total nonfarm payroll: All employees in log levels.	Fred
9	IP	Industrial production index in log levels.	Fred
10	Help to unemp.	Help wanted to unemployment ratio.	Fred
11	Pers. income	Real personal income in log levels.	Fred
12	M&T sales	Real manufacturing and trad sales in log levels.	Fred
13	Earnings	Average of hourly earnings (goods producing) in log levels.	Fred
14	PPI	Producer price index (finished goods) in log levels.	Fred

Note: All for the 1975Q1-2012Q3 period. Monthly series converted to quarterly by averaging over the quarter.

Table G.2 Description of financial variables

	Name	Description	Source
1	Spread	Difference between the 10-year Treasury rate and the FFR.	Fred
2	S&P500	S&P500 stock index in logs levels.	Fred
3	S&P dividend yield	S&P dividend yield, in log and annualized.	Fred
4	EBP	Excess bond premium as computed by Gilchrist and Zakrajšek (2012).	Gilchrist's website (Mar/2015)
5	Excess returns	CRSP excess returns, in log and annualized.	French's website (Jul/2016)
6	SMB	Small minus big risk factor, in log and annualized.	French's website (Jul/2016)
7	HML	High minus low risk factor, in log and annualized.	French's website (Jul/2016)
8	Momentum	Momentum, in log and annualized.	French's website (Jul/2016)
9	R15-R11	Small stock value spread, in log and annualized.	French's website (Jul/2016)
10	Ind. 1	Consumer industry sector-level return, in log and annualized.	French's website (Jul/2016)
11	Ind. 2	Manufacturing industry sector-level return, in log and annualized.	French's website (Jul/2016)
12	Ind. 3	High technology industry sector-level return, in log and annualized.	French's website (Jul/2016)
13	Ind. 4	Health industry sector-level return, in log and annualized.	French's website (Jul/2016)
14	Ind. 5	Other industries sector-level return, in log and annualized.	French's website (Jul/2016)

Note: All for the 1975Q1-2012Q3. Monthly series converted to quarterly by averaging over the quarter.

Table G.3 Macroeconomic and financial uncertainties

	Name	Description	Source
	Financial Uncertainty Measures		
1	Realized Volatility	Realized volatility computed using daily returns using the robust estimator by Rousseeuw and Croux (1993).	CRPS
2	VXO	Option-implied volatility of the SP100 future index. Available from 1986Q1.	CBOE
3	LMN-fin-1	Financial forecasting uncertainty computed by	Ludvigson's
4	LMN-fin-3	Ludvigson et al. (2016). -1 is one-month-ahead, -3 is	website
5	LMN-fin-12	three-months and -12 is one-year ahead.	(Feb/2016)
	Macroeconomic Uncertainty Measures		
1	Policy uncertainty	Economic Policy Uncertainty Index in logs computed by Baker et al. (2016).	Bloom's website (Mar/2016)
2	Business uncertainty	Business forecasters dispersion computed by Bachmann et al. (2013) up to 2011Q4.	AER website
3	SPF disagreement	SPF forecasters dispersion on one-quarter-ahead Q/Q real GDP forecasts computed using the interdecile range.	Philadelphia Fed
4	LMN-macro-1	Macro forecasting uncertainty computed by Ludvigson	Ludvigson's
5	LMN-macro-3	et al. (2016). -1 is one-month-ahead, -3 is three-months	website
6	LMN-macro-12	and -12 is one-year ahead.	(Feb/2016)

Note: All for the 1975Q1-2012Q3 period except when noted. Monthly series converted to quarterly by averaging over the quarter.

H Appendix: Volatilities

Figure 15 Volatilities of macroeconomic variables

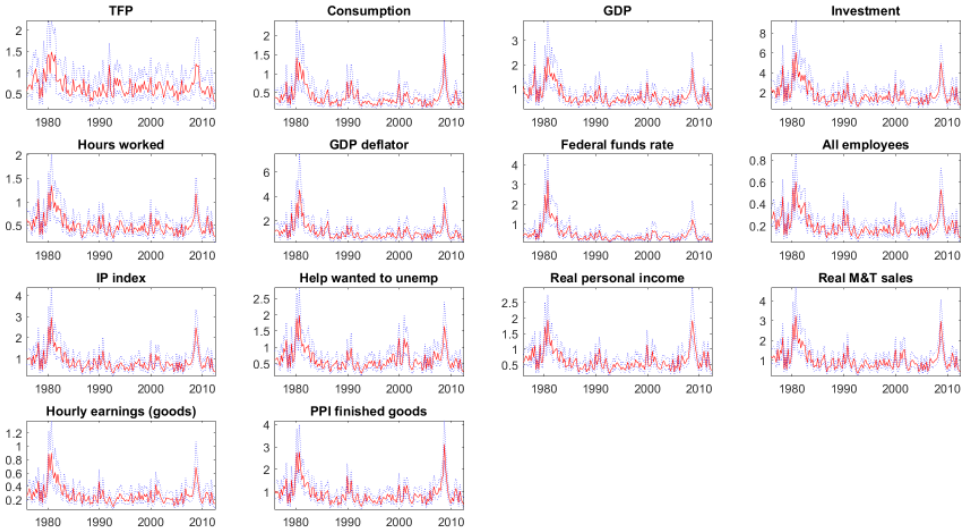

Note: The estimated volatilities of macroeconomic variables are composed of an idiosyncratic component and the common macroeconomic volatility factor weighted by a loading $\beta_{m,j}$. The dotted lines define the 68% confidence bands computed with 200 posterior draws. The macroeconomic variables are described in Table G.1.

Figure 16 Volatilities of financial variables

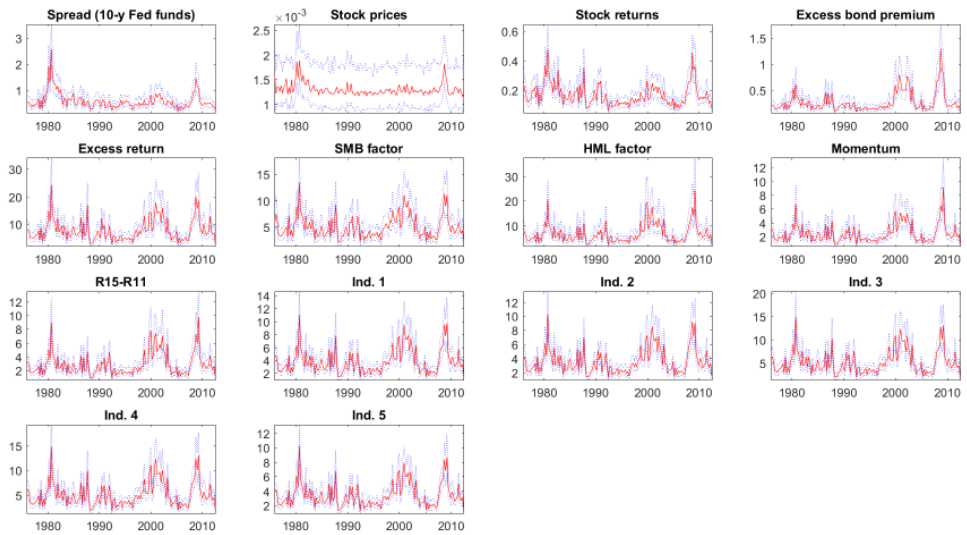

Note: The estimated volatilities of financial variables are composed of an idiosyncratic component and the common financial volatility factor weighted by a loading $\beta_{f,j}$. The dotted lines define the 68% confidence bands computed with 200 posterior draws. The financial variables are described in Table G.2.

I Appendix: Alternative ordering of uncertainty shocks

Figure I.1 Impulse responses to a financial uncertainty shock with financial uncertainty ordered first

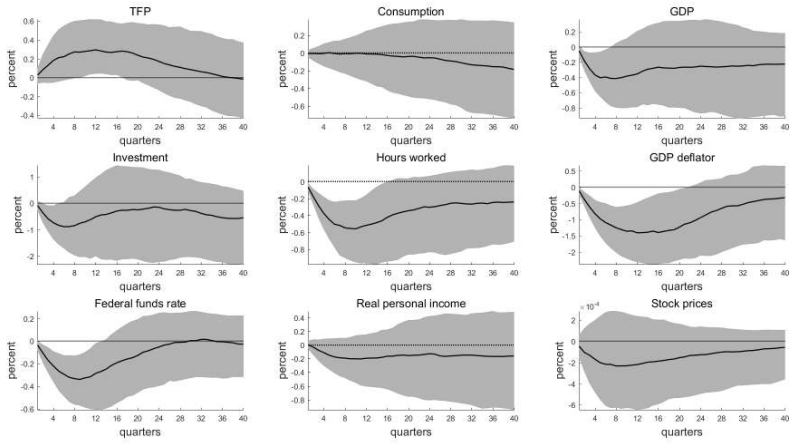

The uncertainty shocks with alternative ordering are identified through Cholesky decomposition with financial uncertainty ordered first, and macroeconomic uncertainty ordered last, as described in Section 3.3. The generalized impulse responses of the uncertainty shock are the average of 1,000 simulated random innovations, as described in Appendix F. The shaded areas define the 68% confidence bands computed with 200 posterior draws.

Figure I.2 Impulse responses to a macroeconomic uncertainty shock with financial uncertainty ordered first

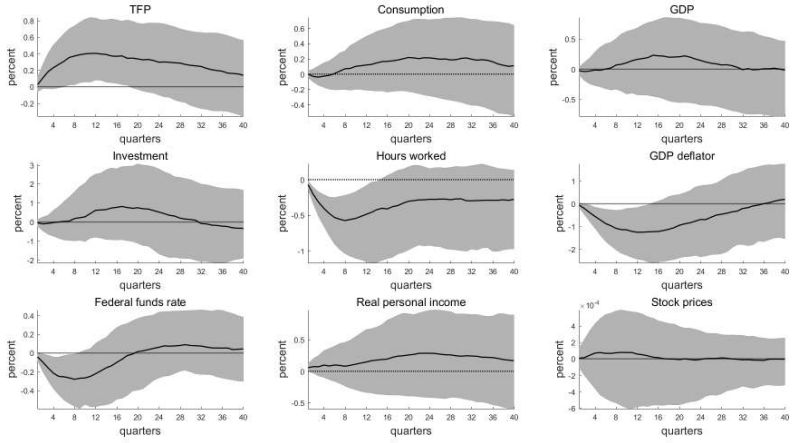

Note: The uncertainty shocks with alternative ordering are identified through Cholesky decomposition with financial uncertainty ordered first, and macroeconomic uncertainty ordered last, as described in Section 3.3. The generalized impulse responses of the uncertainty shock are the average of 1,000 simulated random innovations, as described in Appendix F. The shaded areas define the 68% confidence bands computed with 200 posterior draws.

J Appendix: Full generalized impulse responses

Figure J.1 Time-varying effects of news shocks over different forecast horizons

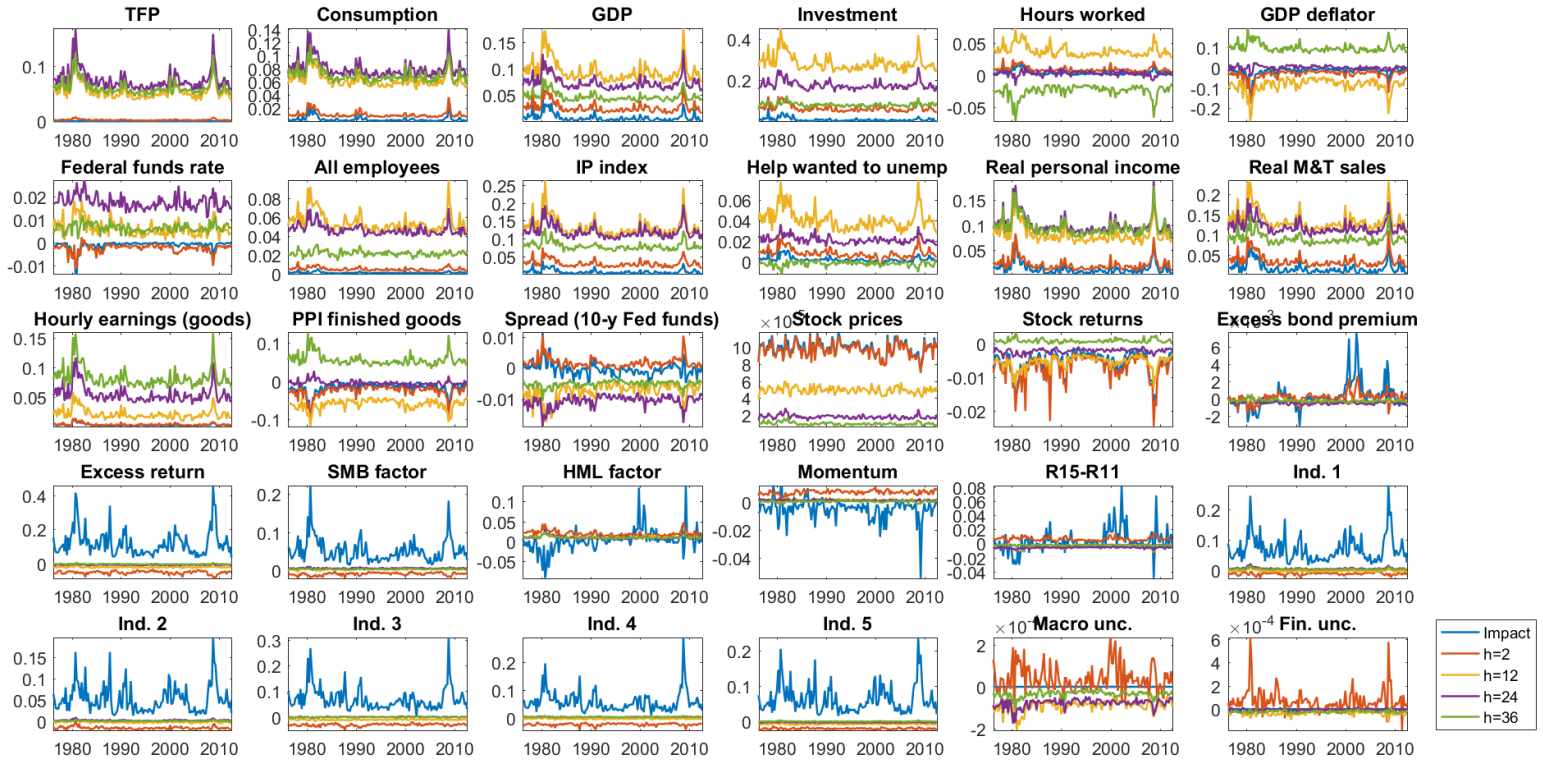

Note: The news shock is identified for each period in time under the procedure proposed in Section 3.1. The generalized impulse responses for each period are the average of 1,000 simulated random innovations, as described in Appendix F. Each line corresponds to the effect of the news shock h-quarters ahead from the point in time.

Figure J.2 Impulse responses to news shocks in periods of high and low macro uncertainty

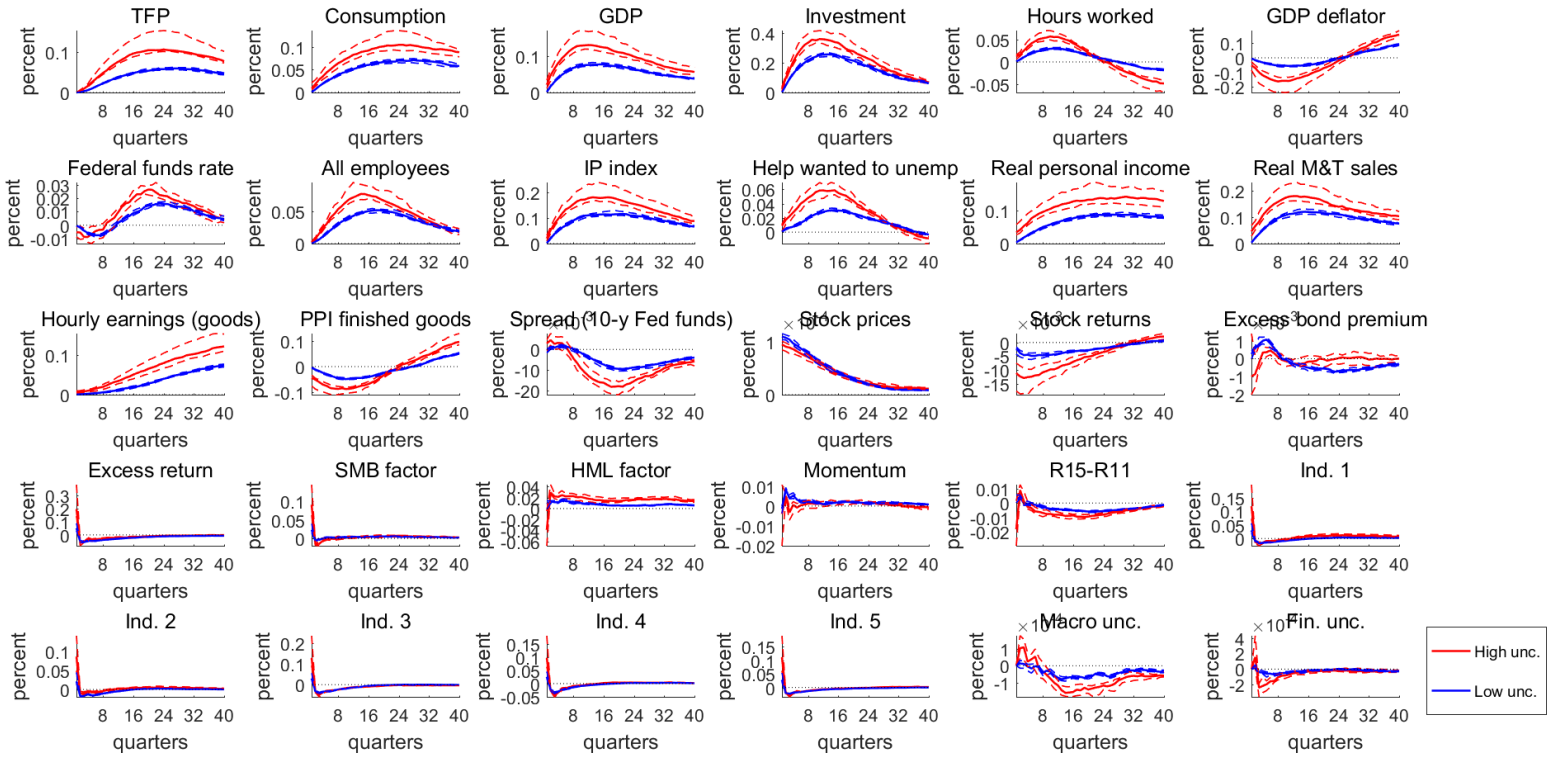

Note: The news shock is identified for each period in time under the procedure proposed in Section 3.1. Red and blue lines correspond to the average of generalized impulse responses on periods of high and low uncertainty, respectively. High and low uncertainty are the periods with the higher and lower 10% values for the macroeconomic uncertainty, respectively. Each impulse response is evaluated at the posterior mean. Dashed lines correspond to 68% distribution of the impulse responses in the high and low periods.

Figure J.3 Impulse responses to a financial uncertainty shock

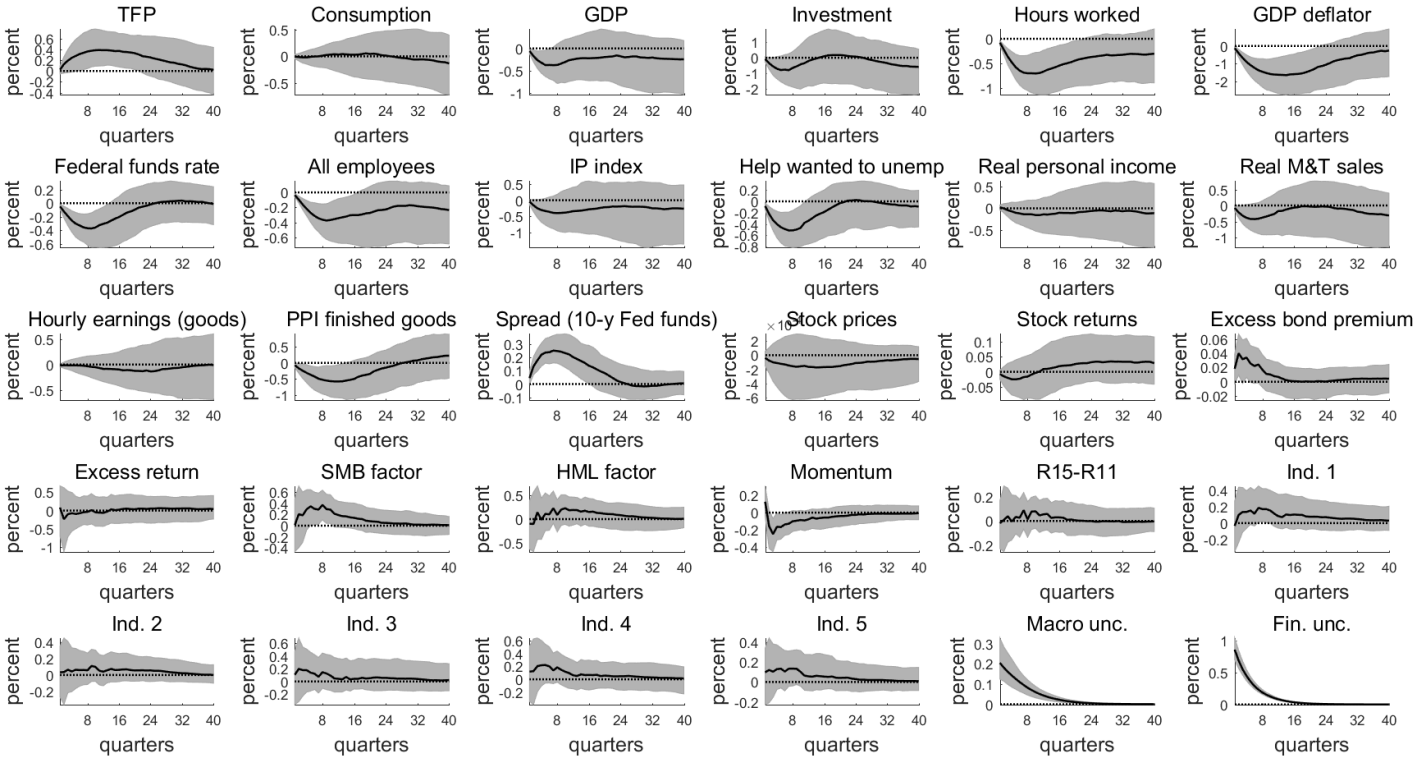

Note: The uncertainty shocks are identified through Cholesky decomposition with macroeconomic uncertainty ordered first, and financial uncertainty ordered last, as described in Section 3.3. The generalized impulse responses of the uncertainty shock are the average of 1,000 simulated random innovations, as described in Appendix F. The shaded areas define the 68% confidence bands computed with 200 posterior draws.

Figure J.4 Impulse responses to a macroeconomic uncertainty shock

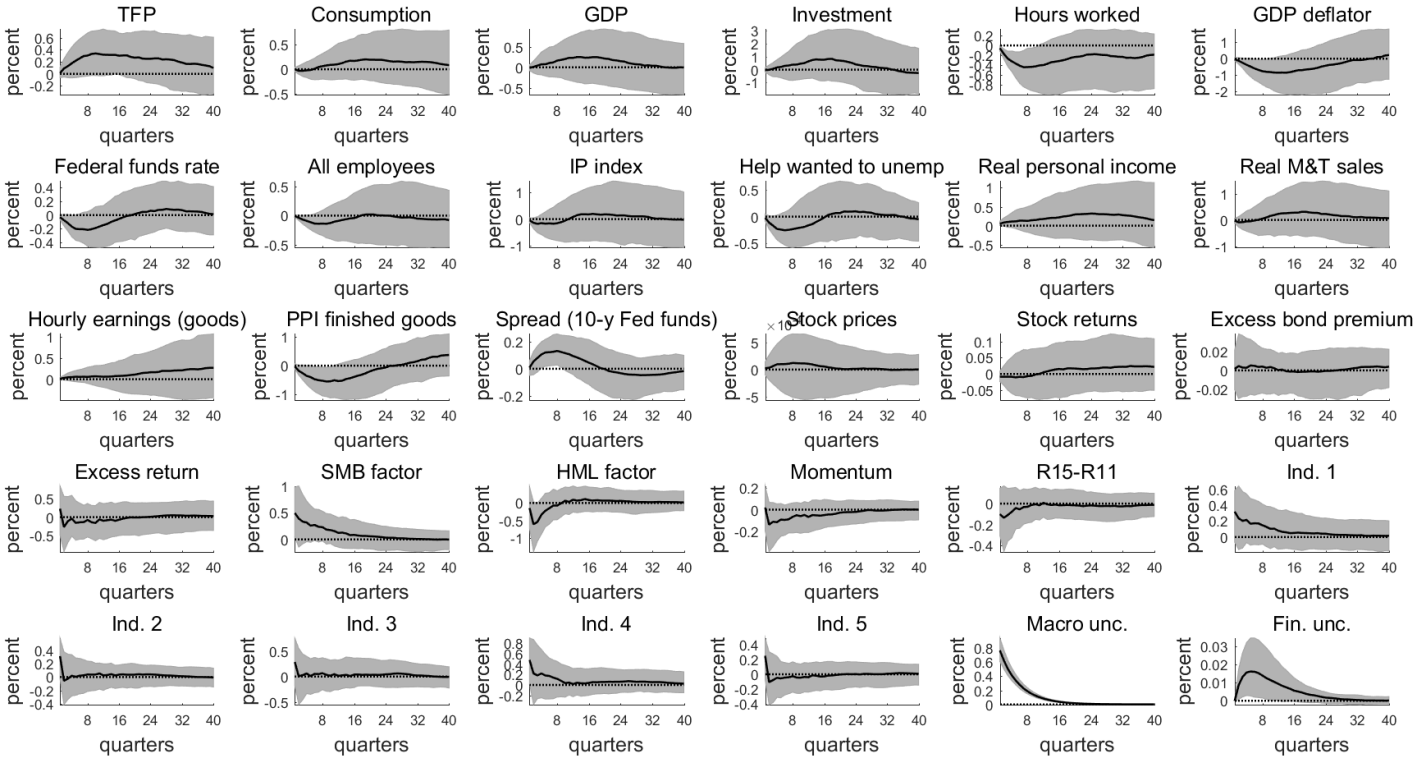

Note: The uncertainty shocks are identified through Cholesky decomposition with macroeconomic uncertainty ordered first, and financial uncertainty ordered last, as described in Section 3.3. The generalized impulse responses of the uncertainty shock are the average of 1,000 simulated random innovations, as described in Appendix F. The shaded areas define the 68% confidence bands computed with 200 posterior draws.

Figure J.5 Impulse responses to a financial uncertainty shock with financial uncertainty ordered first

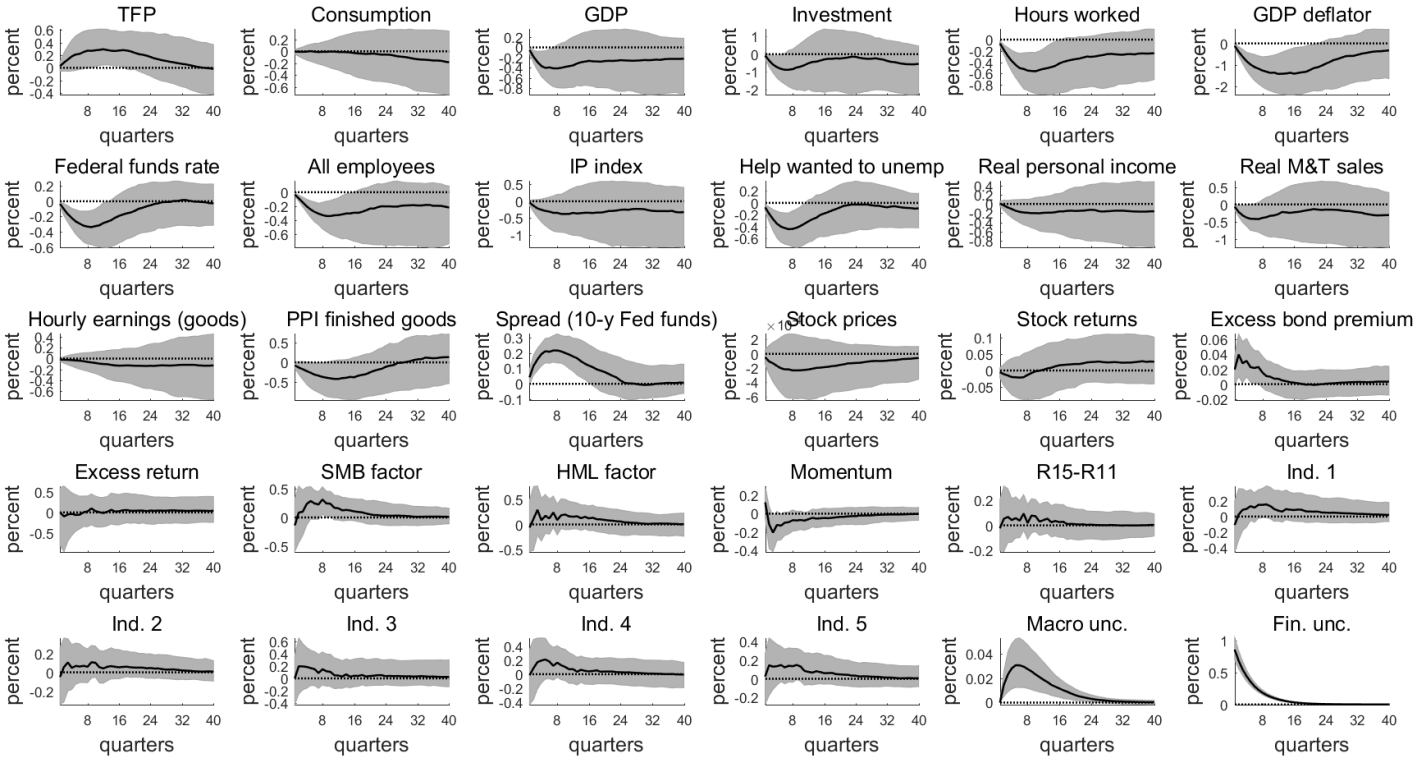

The uncertainty shocks with alternative ordering are identified through Cholesky decomposition with financial uncertainty ordered first, and macroeconomic uncertainty ordered last, as described in Section 3.3. The generalized impulse responses of the uncertainty shock are the average of 1,000 simulated random innovations, as described in Appendix F. The shaded areas define the 68% confidence bands computed with 200 posterior draws.

Figure J.6 Impulse responses to a macroeconomic uncertainty shock with financial uncertainty ordered first

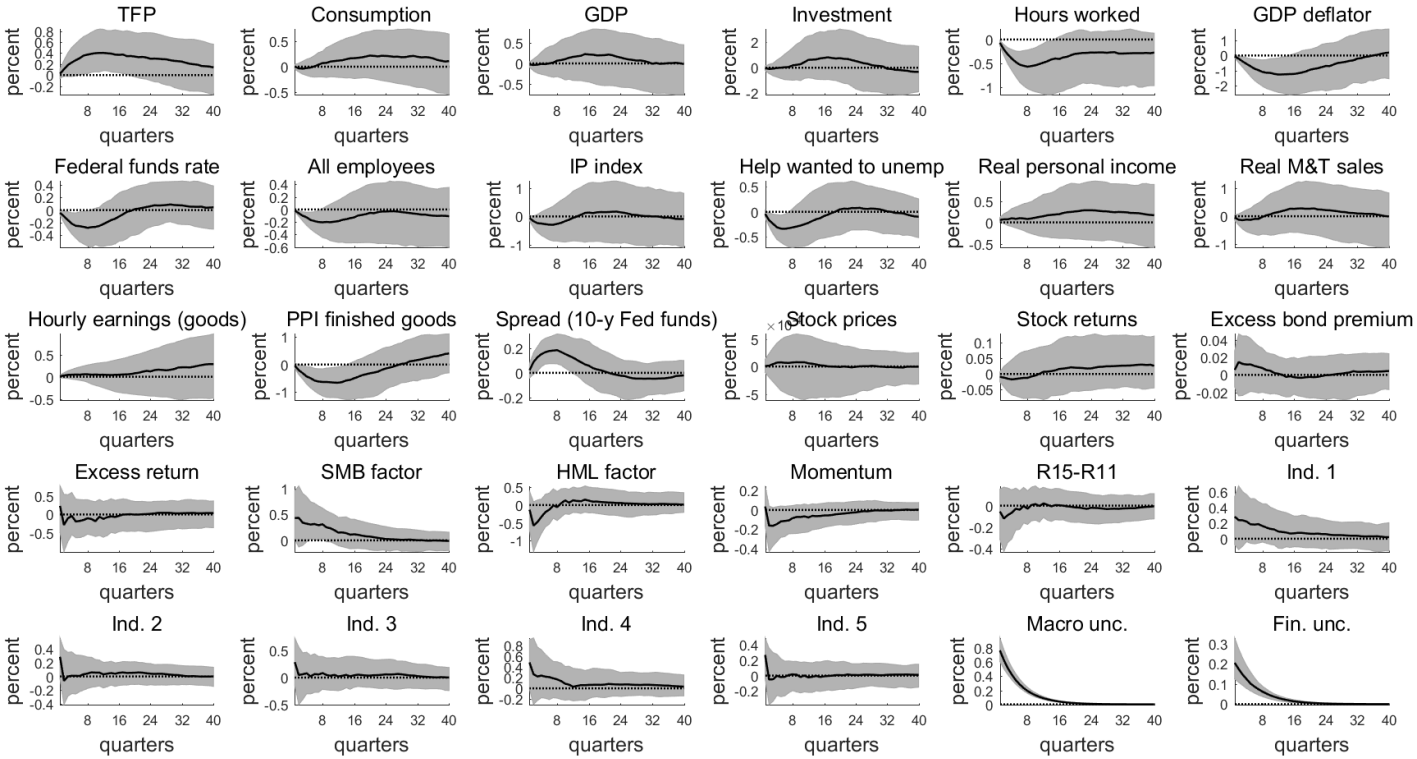

Note: The uncertainty shocks with alternative ordering are identified through Cholesky decomposition with financial uncertainty ordered first, and macroeconomic uncertainty ordered last, as described in Section 3.3. The generalized impulse responses of the uncertainty shock are the average of 1,000 simulated random innovations, as described in Appendix F. The shaded areas define the 68% confidence bands computed with 200 posterior draws.